Environmental Science and Pollution Research
https://doi.org/10.1007/s11356-021-17874-9

RESEARCH ARTICLE

Micro- and mesoplastics in sea surface water from a Northern Adriatic coastal area

Davide Marchetto[1,2] · **Lavinia de Ferri**[3] · **Aurelio Latella**[1] · **Giulio Pojana**[1]

Received: 14 April 2021 / Accepted: 27 November 2021

Abstract

The presence of microplastics in the sea is a global issue widely studied and discussed in the last years. The whole marine ecosystem is now considered at high risk because of their presence and abundance in every studied environment all over the world because polymeric materials commonly constitute the main raw materials in contemporary industrial production. The presented study reports the results obtained from surface seawater monitoring of two sampling transects in the coastal area close to the Venice Lagoon (Italy) inlet, investigated in order to get new information about the presence and relevance of plastic pollution. Plastic particles collected by means of a manta net (0.3-mm mesh size) have been characterized in detail by utilizing a multi-technique approach in order to discriminate them by typology, dimension, colour, spatial density and chemical composition. Such information permitted the individuation of subgroups (specific groups) of plastic micro-debris in this Northern Adriatic area.

Keywords Microplastics · Mesoplastics · Seawater · Adriatic Sea

Introduction

Marine litter generated by anthropic activities represents an additional negative pressure on habitat and resources of all seas (Goldberg 1994, 1995), causing increasing disturbance factors on the functionality of various ecosystems (Laist 1987; Browne et al. 2015). Many items disposed or accidentally dispersed in the marine environment are actually composed by synthetic materials, particularly by plastic polymers. Plastics were introduced in the market only in the last century, but with a huge increase in production and consumption from 1950 (Andrady and Neal 2009), now contributing to over 60% of anthropogenic debris in the marine environment (Derraik 2002) and rapidly becoming a global problem with possible serious implications (Pruter 1987; Moore 2008). Because of the very broad and various fields of application of plastics, their presence in the marine ecosystems can vary both in quantity and quality within a wide range of size, morphology and chemical composition. The plastic litter, once introduced in the environment, is further involved in various processes of distribution, accumulation, degradation and fragmentation (Barnes et al. 2009). Both production and dispersion of plastic litter cause a diffuse accumulation of persistent debris in many terrestrial and marine habitats (Barnes et al. 2009), since these materials are not involved in natural biogeochemical cycles. Plastics are generally subjected to fragmentation processes into smaller fractions persisting in the environment instead of being completely eliminated through mineralization processes (Cooper and Corcoran 2010; Cózar et al. 2014; ter Halle et al. 2016). Degradation processes of plastics in the environment are actually very long (from tenths to hundredths of years), as specifically demonstrated for some biological pathways (Ohtake et al.1998a, 1998b; Mueller 2006). When approaching the problem of degradation of

Responsible Editor: V.V.S.S. Sarma

✉ Davide Marchetto
davidmar@unive.it; jp@unive.it

✉ Giulio Pojana
davidmar@unive.it; jp@unive.it

[1] Department of Philosophy and Cultural Heritage, University Ca' Foscari of Venice, Dorsoduro 3484/D, 30123 Venice, Italy

[2] Department of Environmental Sciences, Informatics and Statistics, Ca' Foscari University of Venice, Venice, Italy

[3] Department of Collection Management-Museum of Cultural History, University of Oslo, Kabelgaten 34, 0580 Oslo, Norway

Published online: 23 January 2022

plastics in the seawater environment, the very short time elapsed since the introduction of synthetic polymers (50's of the last century) must be also taken into account. As cited above, this is connected to the very long time naturally necessary to induce mitigation adaptive responses by biological organisms and ecosystems (Andrady, 2011; Gewert et al., 2015; Pegram and Andrady, 1989; Azzarello and Van Vleet, 1987; Browne et al., 2008a; Green et al., 2017; Gregory, 2009; Lithner et al., 2011; Wright et al., 2013). Concurrently, the socio-economical awareness of sea as a limited natural resource has been developed only recently (Thompson et al. 2009).

Plastics in the marine environment can impact sea life by means of various disturbance processes: plastic macro- and meso-litter, such as shoppers, fishing gear, packaging and bottles, can entangle aquatic animals, hindering or reducing movements or feeding activities until severe injuries or death (Laist 1997; Gregory 2009). The ingestion of plastic fragments may reduce metabolic efficiency of many species because of food substrate dilution or, in the worst case, clogging or tearing the digestive apparatus (Wright et al. 2013). The ingestion of microplastics and their accumulation and transfer along the food chain have already been documented for organisms from various taxa, at different trophic levels and in various ecosystems (Lusher et al. 2013; Farrell and Nelson 2013; Setälä et al. 2014; Van Cauwenberghe and Janssen 2014; Avio et al. 2015; Chae and An 2017). When fragments between hundreds of nanometres and a few millimetres in size ("microplastics", i.e. plastic particles having sizes lower than 5 mm, according to Arthur et al. 2008 and European Commission Joint Research Centre, Institute for Environment and Sustainability 2011) are ingested, additional consequences at histological and cytological level can occur (Browne et al. 2008a; Jeong et al. 2016; Wright and Kelly 2017; Lei et al. 2018; Yu et al. 2018; Hirt and Body-Malapel 2020). When the size falls below few hundreds of nanometres, they can penetrate through organism physiological barriers, affecting and reducing some cellular functions (Browne et al. 2008b; Jeong et al. 2016; Espinosa et al. 2017; Veneman et al. 2017; Ribeiro et al. 2017; Gambardella et al. 2017; Pitt et al. 2018; Jin et al. 2018; Lei et al. 2018).

Some clues that microplastics can act also as vectors for hydrophobic organic pollutants have already been reported (Teuten et al. 2007; Ogata et al. 2009; Engler 2012; Rochman et al. 2013; Bakir et al. 2014).

The presence of microplastics in the marine environment is considered an emerging issue within the environmental quality status in the European Seas: the EU *Marine Strategy Framework Directive*, (MSFD2008/56/EC), Annex I, lists microplastics monitoring among 12 qualitative descriptors selected to evaluate the *Good Environmental Status* of coastal and marine areas to be achieved within 2020 (Galgani et al. 2013).

The Adriatic Sea is an area where pollution due to plastic waste and microplastics is a relevant issue, as also observed for the rest of the Mediterranean Sea (Cózar et al. 2015; Cincinelli et al. 2019). In the frame of a wider project (EU IPA-Adriatic) concerning the presence and impact of plastic litter in the Adriatic basin, the present study aimed to document the status of microplastics pollution in the Northern Adriatic Sea. In particular, surface seawater was monitored in the coastal area close to the Venice Lagoon (Italy) inlet, an area strongly affected by anthropic pressure. The presented study focused on the identification of microplastics and proposed a method for managing and integrating many different sets of data (morphology, visual aspect and chemical nature), as those normally obtained when collecting microplastics from seawater. Each of them can be analysed under various points of view in order to optimize the obtainable information, since all these properties are relevant to define their origins (Helm 2017; Fahrenfeld et al. 2019) and fates (Shaw and Day 1994). Information about shape (ter Halle et al. 2016) and colour (Martí et al. 2020) can integrate data about polymeric compositions, obtained from spectroscopic analysis. Specific combinations of these characteristics can identify or highlight specific degradation pathways (Gewert et al. 2015; Brandon et al. 2016; Lambert and Wagner 2016; Andrady 2017) of plastic particles potentially interacting with the biological components and with effects observable from the molecular (LeMoine et al. 2018; Prokić et al. 2019; Limonta et al. 2019) to the community and ecosystem level (Setälä et al. 2014, 2016b; Green et al. 2016, 2017; Guzzetti et al. 2018; Botterell et al. 2019).

Materials and methods

Sampling site description and meteo-oceanographic information

Monitoring of microplastics on sea surface was performed on October 27 (9:20 a.m.–12:10 p.m.) and December 15 (10:10 a.m.–1:20 p.m.) 2015 in a marine coastal area in front of the Venice Lagoon (Italy). The sampling area is located along the seaward side of southern Lido Island, close to the Malamocco Sea Inlet of the Venice Lagoon. Figure 1 shows location and monitoring tows during the October and December campaigns, labelled as M1 and M2, respectively.

Meteorological information about sea condition during the sampling sessions was acquired by available online databases providing data from four meteo-mareographic stations (Fig. 1). Two stations are located on the northern dam of the Malamocco Sea Inlet (Malamocco Diga Nord, MDN, 45° 20′ 04.02″ N, 12° 20′ 29.85″ E) and on an oceanographic platform (*Piattaforma Oceanografica CNR*, 45° 18′ 51.27″

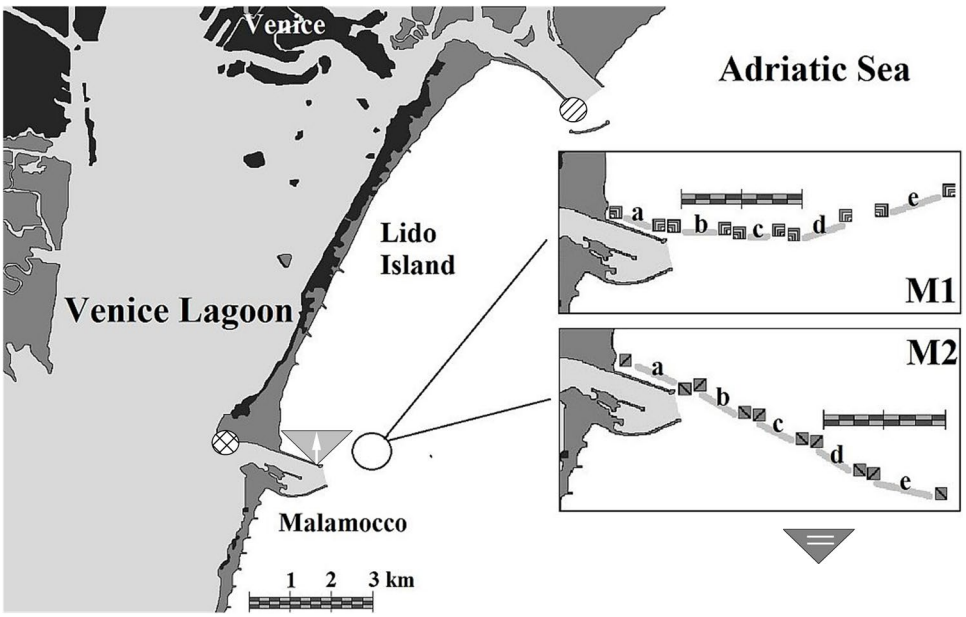

Fig. 1 Map of investigated coastal areas and focus on pathways of monitoring tows during October (M1) and December (M2) campaigns. Location of CNR meteorological stations are indicated by triangles: light grey = MDN, employed for wind and tides data; dark grey = PO-CNR, employed for wind data. Location of ISPRA mareographic station employed for temperature and conductibility data is indicated by a white striped circle

N, 12° 30′ 29.93″ E) at 14.5 km (7.83 nm) from the coastline (https://www.venezia.isprambiente.it/rete-meteo-mareografica). In addition, data were collected from the Faro Rocchetta station (FR, 45° 20′ 21.18″ N, 12° 18′ 39.64″ E) (https://www.venezia.isprambiente.it/rete-meteo-mareografica) and from the mareographic station Lido Diga Sud (LDS), located in the Lido inlet southern dam (45° 25′ 05.59″ N, 12° 25′ 35.50″ E) (https://www.mareografico). Data about wind direction and velocity at 10 m over the ground (U_{10}) were recovered from the same MDN, PO-CNR and LDS stations; data about water temperature and conductivity were collected by the LDS station, while data about tides were available from the MDN and FR stations.

Values of significant wave height (*Hs*) during the sampling were obtained for the fetch and the depth limited waves by means of the on-line *USGS calculator* software (2015), using the algorithms proposed by the *Shore Protection Manual* (United States Army Corps of Engineers and Coastal Engineering Research Center, USA, 1984). Mean wind velocity values based on data from the "PO-CNR" meteo-mareographic station (collected every 10 min in the 6 h previous and during the sampling sessions) were considered for calculation. For the *Hs* calculation, a mean bathymetric depth of 25 m and a fetch of 80 km were considered. These values account for a potential range of the Bora wind, from NE, and the absence of Sirocco wind, from SE at the sampling time.

Data related to water temperature and conductivity within a total time interval of 48 h (including the sampling day and the previous 24 h) was considered to calculate the corresponding salinity values, using the *Conductivity ratio to practical salinity conversion* (SAL78) equation, as recommended by the UNESCO Technical Papers in Marine Science 44—*Algorithms for Computation of Fundamental Properties of Seawater* (Fofonoff and Millard 1983). Finally, water density values at the sampling time were calculated by applying the *Millero-Poisson one atmosphere equation* of state of seawater (Millero and Poisson 1981).

Sampling procedures and estimation of microplastic recovery

Microplastic debris were collected by means of a "Manta" Net trawl specifically designed for continuous-flow sampling of organisms and flotsam at the sea surface (Neuston) (Brown and Cheng 1981). This sampling tool, extensively applied also for sampling of marine litter on the sea surface, consists of a metallic mouth (0.6 × 0.2 m) with buoyant wings, a 300 cm long 0.3 mm mesh bag net with a cod end (Moore et al. 2001; Hidalgo-Ruz et al. 2012) and a calibrated mechanical flowmeter (HYDRO-BIOS GmbH, Warburg, Germany) mounted on the internal part of the mouth in order to measure the real seawater volume flowing through the net. As recently reported (GESAMP 2019; Michida et al. 2019), the use of a flowmeter during sampling of microplastics is strongly recommended.

Two transects on sea surface about 6200 m long (3.34 nautical miles, nm) were monitored starting at 140 m from Lido Island shoreline and moving perpendicularly to the coastline toward the open sea. Each transect consisted of 5 tows, performed at 1–2 kt (0.51–1.03 m/s) speed with a sampling time of approx. 30 min, leading to individual paths measuring about 926–1852 m (0.5–1 nm). All data related to geographical coordinates, row lengths (Eq. 1S in Supplementary Information, SI), seawater volumes (Eq. 2S in SI) and sampled area lengths were collected during each tow

(Table S1 in SI). Transect 1 (indicated as M1 in Fig. 1) was sampled in October 2015, while transect 2 (indicated as M2 in Fig. 1) in December 2015.

An assessment of the total number of plastic fragments (N) at the wind-mixed surface layer was obtained from an estimation of particles lost during sampling and distributed along the water column depth under the manta-net mouth. The N values were calculated using the model described by Kukulka et al. (2012) and extensively applied in microplastic monitoring studies (Reisser et al. 2013; Cózar et al. 2014; Suaria et al. 2016) (Eq. 1).

$$N = \frac{N_{tow}}{1 - e^{-dw_b A_o^{-1}}} \quad (1)$$

where N = number of microplastic particles per km^2 integrated on the water column depth, N_{tow} = number of microplastic particles per km^2 for each Manta net tow, d = immersion depth of the surface-towed net, equal to 0.2 m (full immersion of the net frame), w_{b} = buoyant rise velocity of marine plastics, equal to 0.0053 m s^{-1} (Reisser et al. 2013) and A_{O} = near-surface turbulent exchange coefficient, calculated according to Eq. 2:

$$A_o = 1.5 u_w k H_s \quad (2)$$

where $k = 0.4$ (von Karman constant), H_{s} = significant wave height (m) and u_{w} frictional velocity of water (m·s^{-1}) and calculated as Eq. 3:

$$u_w = \left(\frac{\tau}{\rho_w}\right)^{\frac{1}{2}} \quad (3)$$

where $|\tau| = \rho_a C_D U_{10}^2$ = sea surface wind shear stress, being ρ_{w} = sea water density (1027.5 kg m^{-3}, for a $T_{\text{water}} = 18\text{C}^\circ$ and salinity = 38 psu), ρ_{a} = air density (1.3 kg m^{-3}), C_{D} = drag coefficient (Large and Pond 1981; Trenberth et al. 1990) and U_{10} = wind velocity at 10 m from ground (m·s^{-1}). From Eq. 1, a correction factor (N/N_{tow}) and the recovery efficiency, as percentage of expected value ($N_{\text{tow}} = \%\ N$), were also calculated.

Sample treatment, meso-/microplastic determination, particle image analysis and shape and size measurement

Samples collected from the cod end were sieved at 5 mm mesh under a distilled water flow in order to remove larger debris and to recover mesoplastic particles (MeP, 5–10 mm,), which were then stored in an ethanol/water solution (2:1, v:v) until analysis. Stored samples were further fractionated into two sub-samples by passing them sequentially through 1 and 0.3-mm mesh sieves, respectively, under distilled water flow in order to separate large microplastic particles (LMP, 1–5 mm) from small microplastic particles (SMP, 0.3–1 mm) (Hidalgo-Ruz et al. 2012; Michida et al. 2019).

The microplastic particles collected on the 1-mm sieve were later manually separated from natural debris (such as shell, wood and algae) using tweezers under stereomicroscope inspection. The remaining finest fraction recovered from the 0.3-mm sieve consisted mainly of extracellular microalgae exudates and decomposing organic matter, potentially embedding collected plastic particles. This was digested overnight with a 30% w/v H_2O_2 (Carlo Erba Reagents) solution at 50 °C. Processed samples were then inspected under a stereomicroscope to remove visible plastic items, while the residue was filtered on a glass fibre filters (GF/F; pore size: 0.7 µm) in order to recover the smallest particles. The isolated plastic particles were finally picked up from filters with small Adson tweezers and placed on a customized multiwell with a 0.3 mm metallic net for chemical characterization by spectroscopic methods.

High-resolution (HR) images of microplastic particles were acquired by a D800e Nikon (Minato, Tokyo, Japan) digital camera equipped with a full-frame (24 × 36 mm) 36 Mp CCD sensor and a Contax (Oberkochen, Germany) Makro-Planar 100 mm f/2.8 lens. The camera/lens system was operated at ISO100, f8 aperture and shutter speed between 1/2 and 1/16 s. A LED light source at 5500 K filtered through a dispersion ring around the sample holder was used in order to generate a diffuse illumination and to avoid bias on the microplastic image, due to the formation of shadows. The camera was placed on a macro repro stand, with adjustable heights from the work plane and tethered from PC via the software "Camera Control Pro2" by Nikon. Samples were put on a 100 × 100 mm millimetric reference grid for size determination. All images were calibrated through the Color Checker Passport (X-Rite, Grand Rapids, MI, USA) allowing both white and colour balance (McCamy et al. 1976). The colour of collected microplastics was defined as reported in Hanke et al. (2013) and Shaw and Day (1994).

The acquired HR images were used to obtain detailed information about size and shape of the collected microplastics via the open source image processing software *ImageJ* Ver. 1.46 and an Intuos Photo graphic tablet (Wacom, Saitama, Japan). Each item contour was manually bordered to overcome limitations of automatic contour recognition such as the heterogeneity of colours, shapes and the variable contrast between particles images and the millimetric grid background. The metric dimension scale was set for each particle by converting the unit of measure from pixel to millimetre by using the reference grid of the sample holder (Ferreira and Rasband 2012). All dimensions were measured using the Best Fitting Ellipses Axes function of ImageJ (Gauci et al. 2019).

The acquired HR images were used also for the classification of particles, applying a protocol previously proposed by the literature (Hanke et al. 2013), defining collected fragments as *films*, *pellets*, *foams*, *filaments* and *unclassified particles*). The amount of each class of microplastics was counted as both number of particles per unit of area ($Np \cdot Km^{-2}$) and number of particles per unit of volume ($N_p \cdot m^{-3}$).

Each collected particle was classified also based on its colour and visual aspect (*opaque*, *semi-translucent* and *translucent* or *transparent*), which was evaluated by developing a procedure based on the ability of light to pass through both the examined item and a reference image (a grid with lines of different colours). The criterion was stated following the below procedure: opaque objects are not over-passed by light, and hence the reference image is completely hidden, whereas the transparent objects are easily crossed by light and the reference grid results entirely readable. The semi-translucent objects can be partially passed by light but not by the reference image; finally, the translucent objects can be partially traversed by light, while the reference image is only barely visible and creates a sort of "ghost-image".

Polymer identification

The chemical composition of collected microparticles was determined by three spectrophotometric techniques: Raman spectroscopy (RS), near infrared (NIR) and Fourier transform infrared in attenuated total reflection mode (FTIR-ATR).

Raman spectroscopy was performed to identify the polymeric composition of SMP (0.3–1 mm) and LMP (1–5 mm) by using a BWS415 i-Raman 785S spectrometer coupled with a dedicated optical microscope BAC151B Raman Video Microsampling System, both by B&W Tek Inc. (Newark, DE, USA) by means of optical fibre (1.5 m length) ending in a BAC102 Raman Trigger Probe equipped with a standard 304SS shaft mounting a flat quartz window. The Rayleigh radiation was blocked by a notch filter, and the backscattered Raman light was dispersed by a holographic grating on a TE Cooled Linear 2048 pixels CCD Array (cooling temperature: 10 °C); the entrance slit width was fixed at 25 µm. The microscope has been equipped with a 40 × objective. The laser excitation source consists of a 785-nm diode which power can be modulated (1% steps; maximum power: 300 mW) to avoid thermal effects on the analysed sample. Spectra were collected in the 175–3000 cm^{-1} spectral range, with a nominal spectral resolution of 4.5 cm^{-1} and with typical integration times of 60 s. Five accumulation cycles were collected for each spectrum in order to improve the signal-to-noise ratio. Data collection and management was performed employing the dedicated BWSpec4 software (B&W Tek Inc.). A customized multiwell 0.3-mm metallic net was employed for SMP analysis, while a quartz microscope slide was used as sample holders for LMP.

The SMP were analysed also through a Scimitar 1000 FT-IR spectrophotometer (Varian Inc., Palo Alto, CA, USA) working in attenuated total reflectance (ATR) mode with a diamond-coated ZnS crystal and acquiring in the 600–4000 cm^{-1} spectral range. Both the background and the sample were acquired averaging 64 scans at a spectral resolution of 4 cm^{-1}.

The composition of collected LMP (1–5 mm) was determined by using a near infrared (NIR) (Blanco and Villarroya 2002) handheld spectrometer PhazirTM1624 by Thermo Fisher Scientific Inc. (formerly Polychromix), working in diffuse reflection mode in the 6266–4173 cm^{-1} (1596–2396 nm) spectral range and with a spectral resolution of 19 cm^{-1} (Sorak et al. 2012). The NIR spectrometer consists of a MEMS-based DTS (Digital Transform Spectroscopy) system, where the spectrum collected from the investigated sample, illuminated by a tungsten light source, is dispersed across a diffractive MicroElectroMechanical System (MEMS) chip. A single InGaAs photodiodes detects the near infrared component of the radiation (Geller 2007). The identification of synthetic polymers was carried out by means of the instrument software chemometric method (Blanco and Villarroya 2002) coupled to a proprietary spectral library.

Comparative analysis of plastic particle assemblage structure

All data concerning polymeric compositions (pl.), shape categories (ct.), colours (cl.) and optical properties (op.) were used to create a reference database and combined to assign each micro- and meso-plastic particle to a specific group sg_i {pl.; ct.; cl.; op.}, in order to allow a synoptical approach in the analysis of the floating ensemble structure (some examples of obtained groups are reported in Table S3 in SI).

Both Shannon (entropy index *H'*, Shannon 1948) and Simpson indexes (diversity index D_s, Simpson 1949) were calculated in relation to the proportional abundance of plastic micro- and mesodebris classified according to the sg definition. They allowed quantifying the differences between microplastics sampled in different campaigns.

The Shannon index (or Shannon Entropy) *H'* quantifies the uncertainty associated with the prediction of which plastic debris type can be found in the marine monitored area and can be calculated by means of Eq. 4:

$$H' = -\sum_{i=1}^{SG} p_i ln p_i \quad (4)$$

where $p_i = n_i / N$ represents the portion of plastic particles belonging to the i^{th} sg (n_i) and *N* is the total amount of particles; consequently, if all particles would be associated

to a single sg_i, the H' value is 0, while if all plastic particles would be equally spread in all sg_is, the H' value would be 1/lnSG, where SG represents the total number of encountered sg_is. This value is defined as H'_{max} and it was used to calculate the evenness index, $E_{H'}=H'/H'_{max}$, which allowed evaluating the distribution homogeneity of detected particles in various sgs in M1 and M2.

D_s represents the probability that two randomly sampled particles belong to two different sg, and it is equal to $D_s=1-I$, being I the Simpson Dominance Index, which indicates the probability that two particles randomly sampled from a selected dataset (M1 or M2 in this case) represent the same sg. It can be calculated by Eq. 5:

$$I = \frac{\sum_{i=1}^{SG} n_i\left(n_i - 1\right)}{N(N-1)} \tag{5}$$

where n is the number of particles within a sg_i and N is the total of particles for each sampling campaign (M1 and M2). The D_s^{max} value, that represents the maximum value reachable by the Simpson Index D_s, can be calculated using the relation $1-(1/SG)$, considering all particles as being evenly distributed in all obtained sg_is, with SG being the total number of encountered sg_is. This parameter was utilized to estimate a further evenness index E_{Ds} by calculating the D_s/D_s^{max} ratio. This value would tend to 1 when a maximum evenness degree is observed.

Variances of H' and D_s were estimated by means of Eqs. 3S and 4S, respectively (Brower et al. 1998) reported in SI.

The H' and D_s values obtained for M1 and M2 sampling sessions were compared, and a two-tail t-test was performed to assess the diversity of achieved results. The t-value (t) of each dataset and the degree of freedom (df) for H' and D_s were calculated by means of Eqs. 5S, 6S and 7S, respectively (Jayaraman 1999), reported in SI. Student t referring value was calculated by means of the Student t-Value Calculator (Soper 2018).

Results and discussion

Evaluation of the sampling conditions

The total length of examined transects were calculated by GPS coordinates, resulting in 5.6 km (3 nm), with tows average values of 1.1 ± 0.2 km (0.60 ± 0.11 nm) for the October campaign (M1) and 6.1 km (3.3 nm) for the December one (M2). In this case, the tows average length was 1.1 ± 0.2 km (0.66 ± 0.05 nm) (Table S1 in SI). The bathymetric slope of the transects, from the shoreline to the open sea, was between −2 and −20 m. The coastline in front of the investigated area is composed of sand beaches, limited in the back by natural lines of sand dunes.

Data acquired from the mechanical flowmeter allowed the correct calculation of the filtered water volume. A comparison between flowmeter data and water volumes calculated in the "Sampling procedures and estimation of microplastic recovery" section indicates that filtered water volume actually measured by the flowmeter were always lower than those resulting from calculations based on lengths of the transects' rows. In detail, the volumes sampled in M1 and in M2 represented 62% ± 6% and 81% ± 6% of calculated values, respectively. These percentage values correspond to 441 and 583 m^3 of filtered water, with mean tow volumes of 82 ± 18 and 117 ± 6 m^3 for the first and second sampling session, respectively.

Calculations of the mixing layer depth were performed considering that the mean U_{10} (6 h) for PO-CNR station was 3.1 ± 0.4 ms^{-1} in the former field campaign (M1) and 1.7 ± 0.4 ms^{-1} in the latter one (M2). These wind speed data allowed for estimating significant wave height values (H_s) of 22.1 cm (M1) and 5.4 cm (M2), respectively.

The U_{10} magnitude values for the MDN station, closer to the coastline and to the sampling sites, were acquired as well to assess the wind effect on the efficiency and reliability of debris collection. The wind parameters can have a quite strong impact on the mixing of water surface layers during sampling (Kukulka et al. 2012; Reisser et al. 2013; Michida et al. 2019) (Fig. 2; data related to the 24 h are reported in Fig. 1S). Values ranged between 3.0 and 3.6 ms^{-1} in October (M1) and 0.2 and 2.0 ms^{-1} in December (M2), being these the minimum and maximum average values for tows of each campaign. Drag coefficient values (C_D) of 1.14×10^{-3} for M1 and between 21.8 and 14.2×10^{-3} for M2 were consequently calculated.

The model proposed in the "Polymer identification" section allowed for calculating the proportion of recovered microplastic particles as a function of their theoretical dispersion due to a wind-mixed surface layer. The modelling results are reported as percentages of particles actually sampled in each tow vs. their expected amounts without depth spreading. It was found that recovery efficiencies ranged between 84.5 and 89.3% in M1, while recovery was 100% in M2 due to the absence of wind during this sampling campaign.

Tide data acquired by both MDN and FR platforms were used to clarify any potential contribution of the tide on microplastic distribution in the sampled transects. Outgoing tide situations with a potential water flow from the Venice lagoon to the Adriatic Sea through the inlet were more evident in October than in December (Fig. 3). For sake of completeness, also data acquired by the LDS platform is displayed, since the water temperature and conductivity data used to calculate water salinity and density values were

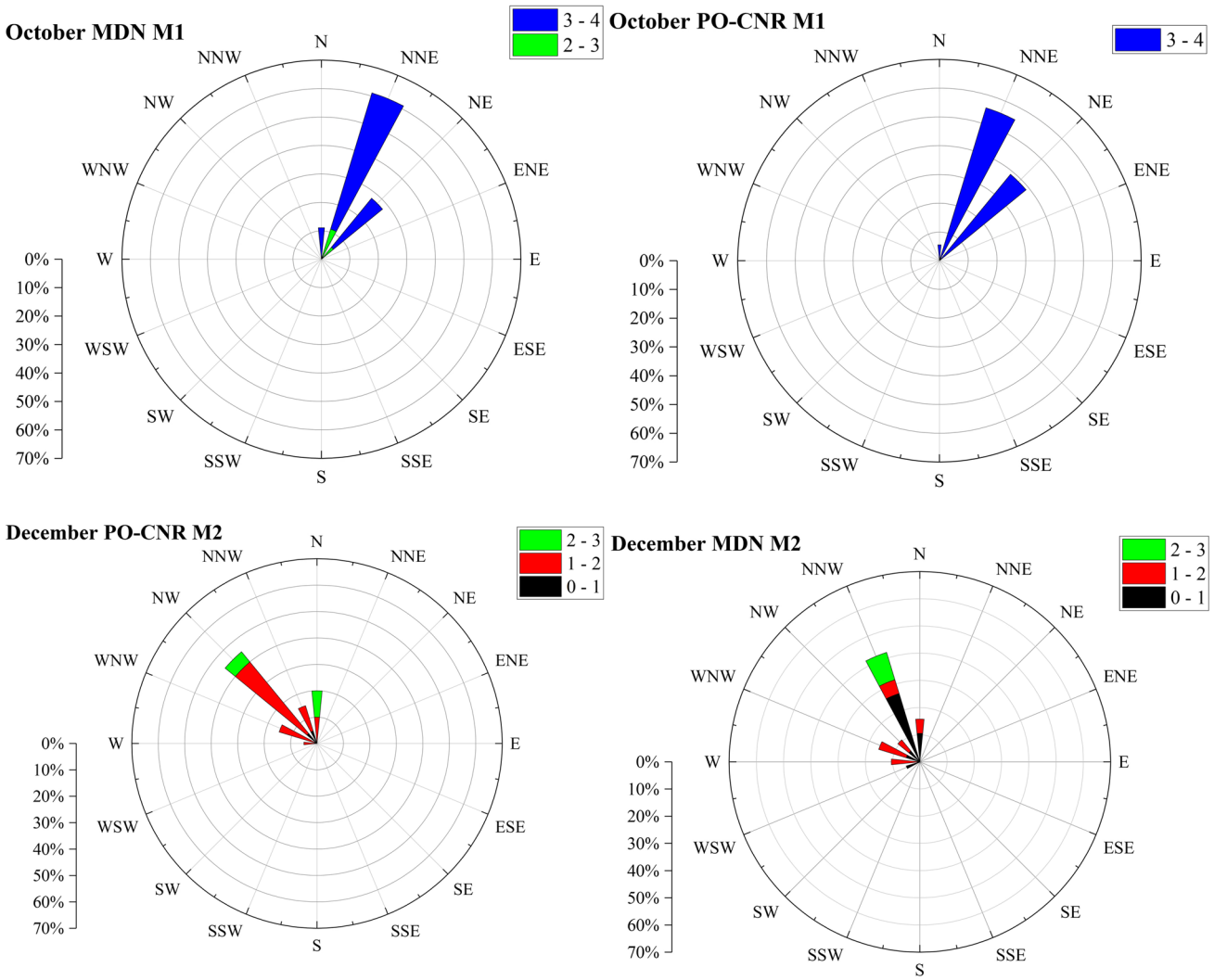

Fig. 2 Wind roses for M1 and M2 periods built on U_{10} wind data collected by the MDN and PO-CNR meteo-mareographic stations [2 columns]. Numbers in the legend represent the wind speed in m/s

collected from the same station. This station is located about 11 km from the starting point of the sampling transects, as well as the MDN and PO-CNR stations. Tide data reported in Fig. 3 clearly show that variations in the considered 48 h always remained lower than 1 m, with a maximum tidal range amplitude of about 80 cm during M1 and of 50 cm during M2. These values fall in the ordinary tidal range amplitudes normally observed in the Venice Lagoon where water exchanges with the Adriatic Sea are mainly driven by tidal flow (Bellafiore et al. 2008).

Salinity values calculated at ~ 16.1 ± 0.2 °C during M1 was found to be ~ 34.6 ± 0.1 psu, while during M2, it was found to be approx. 37.31 ± 0.04 psu when considering an average temperature of approx. 8 ± 1 °C. The average water salinity values reported in the literature for the central lagoon area close to the Malamocco inlet reflect typical marine conditions (Zirino et al. 2014). Salinity values obtained from data available at the LDS station seem to confirm such general conditions, excluding any contribution by fresh and brackish water during sampling campaigns. As shown in Fig. 3, salinity values do not change significantly during each sampling campaign.

As concerning the average density of seawater, slightly different values were found between M1 and M2, being 1025 and 1029 kg/m^3, respectively. Such differences can be related to the already mentioned modifications in terms of water temperatures and salinity between the two campaigns (Fig. 3).

Despite the differences found in the two campaigns regarding the recovery efficiency of microplastics and sampled water volumes, the sea meteorological conditions (wind speed and direction, tide, salinity and water density) allowed to conduct both M1 and M2 in favourable circumstances, with wave height under 50 cm (22 cm in M1 and 5 in M2)

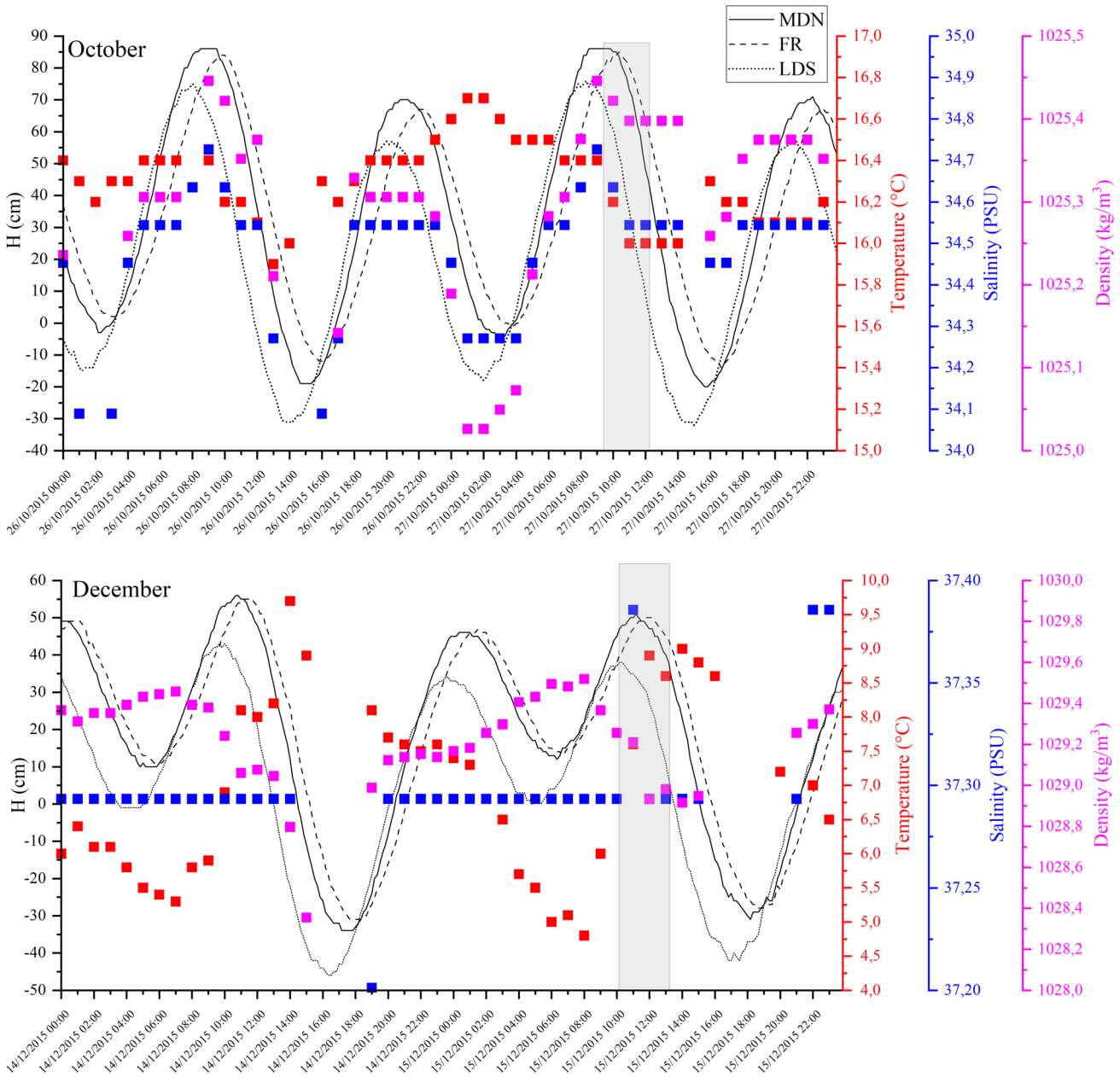

Fig. 3 Tides (cm), temperature (°C), data collected during the 48 h by the MDN, LDS and FR meteo-mareographic stations. Salinity (PSU) and density (kg/m^3) values calculated on the basis of conductivity and temperature data acquired by the LDS station. Grey areas highlight the sampling periods

and wind under Beaufort force scale 3 (2–3 in M1 and 1–2 in M2) (GESAMP 2019; Michida et al. 2019). The differences in the results obtained in M1 and M2 can be evaluated on the basis of seasonal evolutions in the Northern Adriatic circulation system, as reported in the "Currents and circulation in the Northern Adriatic Sea" section.

Higher concentrations of natural organic debris on the sea surface could have affected the water volume sampled during the M1 campaign through a partial net clogging (see the "Microplastic areal density determination" section).

Microplastic areal density determination

The meso- and microplastic particle areal densities were estimated according to information provided by the flowmeter. The overall areal densities are reported as number

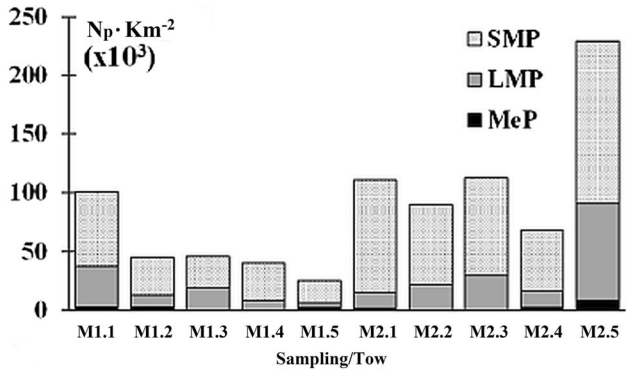

Fig. 4 Areal density, expressed as $N_p \bullet km^{-2}$ ($\times 10^3$), of each sampling tow in M1 and M2 sampling transects

of particles per unit area ($N_p \bullet km^{-2}$), deriving from actual counts of small, large and mesoplastic particles collected at Malamocco Sea Inlet during the sampling activities in M1 and M2 (Table 1).

Data obtained from the two sampling transects (M1 and M2) are reported separately as well as averaging all 10 tows (Mt), specifying results referable to the whole dimensional interval (0.3–10 mm) and to the SMP, LMP and MeP classes. The mean values (51.4×10^3 and 121.9×10^3 for M1 and M2, respectively) and the median values of areal density (44.9×10^3 and 110.8×10^3 for M1 and M2, respectively) pointed out that the number of particles more than doubled in the short time interval elapsed between M1 and M2 monitoring campaigns.

The consistency of differences between M1 and M2 mean data was statistically verified through the non-parametric Mann–Whitney U test ($\alpha = 0.05$, $p = 0.037$), after performing the Kolmogorov–Smirnov-Liliers normality test on data distributions, suitable for small sets of data, which indicated that the normal distribution hypothesis had to be rejected ($\alpha = 0.05$, $p_{M1} = 0.022$ and $p_{M2} = 0.031$). A significant difference between the average values of M1 and M2 areal density data emerged from the parametric t-test ($\alpha = 0.05$, $p = 0.036$).

The contribution of SMP to the total density of plastic particles was prevailing and amounted to approx. 67 and 72% for M1 and M sampling sessions, respectively, whereas particles over 5 mm (MeP) represented the smallest fraction, with values between 2 and 3% (M2-M1).

Ratios between the highest and the lowest observed value for all dimensional classes (range column in Table 1) were 4 for M1, 3.3 for M2 and 9.2 for the overall measurement (Mt), respectively.

The IQR/range (where IQR = interquartile range), expressed as percentage, allowed to estimate that the interval between 25 and 75% percentile of observed data fell within narrow intervals of areal density values, when considering the total amount of recovered plastic particles. The percentage ratios were approx. 8 and 14% of measured density range in M1 and M2, respectively. Some variations with respect to these areal densities were observed when other size classes were considered.

In order to evaluate the distribution symmetry, the ratio (median-min.)/(max.-median) and the skewness coefficient were calculated: ratio values of 2.7 and 2.8 were found, while the skewness coefficients amounted to 0.66 and 0.15, for M1 and M2, respectively. These results pointed out that a positive asymmetry exists for sample distribution, also evidenced by the data distribution (Fig. 4, Table 2aS, 2bS). This assessment allowed to state that plastic particle areal density magnitudes were comparable within tows of the same transect, except for the singular "hotspot" tows M1.1, being the nearest to the shoreline, and M2.5, being the farthest (Tables S2a, b in SI).

The comparison of observed data through the Kolmogorov–Smirnov test indicated that it was not possible

Table 1 Descriptive statistics of data collected during M1 and M2 campaigns and average of the overall data Mt ($N_p \bullet km^{-2}$ ($\times 10^3$)). Range of particles collected in each transect with details for the three size categories (min–max values); average values (confidence interval 95%) and median (1st–3rd quartile); ratio between the interquartile range (IQR = 3^{rd}Q-1^{st}Q) and the corresponding range value. The percentage of particles was calculated for each size class considering average values ($N_p \bullet m^{-3}$ can be obtained as $N_p \bullet km^{-2}$ ($\times 5.1 \bullet 10^{-6}$)). Bold= full size range (0.3-10 mm)

	Size	%	Range (min.–max.)	Average	Median	IQR/range
	mm			$N_p \bullet km^{-2}$ ($\times 10^3$)		(%)
M1	**0.3–10**		**25.0–100.6**	**51.4 (15.7–87.1)**	**44.9 (40.2–46.3)**	8.0
	0.3–1	67.3	18.8–63.3	34.6 (13.6–55.6)	31.6 (27.0–32.5)	12.3
	1–5	29.8	4.2–34.5	15.3 (0.3–30.3)	10.0 (8.6–19.3)	35.2
	5–10	2.9	0–2.9	1.5 (0–3.2)	2.1 (0–2.5)	86.8
M2	**0.3–10**		**68.3–229.0**	**121.9 (44.4–199.5)**	**110.8 (89.5–112.2)**	14.1
	0.3–1	71.6	52.1–138.4	87.3 (46.4–128.1)	82.4 (67.5–95.9)	32.9
	1–5	26.5	13.2–82.4	32.3 (0–68.0)	22.0 (14.4–29.8)	22.3
	5–10	1.9	0–8.2	2.3 (0–6.6)	1.7 (0–1.8)	21.8
Mt	**0.3–10**		**25.0–229.0**	**86.7 (44.5–128.9)**	**78.9 (45.3–108.2)**	30.9
	0.3–1	70.3	18.8–138.4	60.9 (34.4–87.5)	57.7 (31.8–78.7)	39.2
	1–5	27.5	4.2–82.4	23.8 (7.6–40.0)	16.8 (10.8–27.8)	21.8
	5–10	2.2	0–8.2	1.9 (0.1–3.7)	1.7 (0–2.4)	29.1

to refuse the hypothesis that both M1 and M2 exhibit the same sample distribution ($\alpha = 0.05$, $p = 0.082$). The overall average Mt value resulted in 86.7×10^3 $N_p \bullet km^{-2}$, while the median is 78.9×10^3 $N_p \bullet km^{-2}$ (Table 1), as shown in Fig. 5, also displaying how each size class (SMP, LMP and MeP) accounted for 84, 14 and 2% of total particles sampled, respectively. As resulted from the Kolmogorov–Smirnov test ($\alpha = 0.05$ and $p = 0.644$) and shown in Fig. 5, Mt data followed a normal distribution with a positive skewness (calculated coefficient = 0.14).

These values were significantly different from a statistical point of view; however, they did not indicate any relevant difference about the plastic pollution conditions between M1 and M2.

Based on the most recent literature updates, data about the areal density of smallest particles (> 1 mm) should be carefully evaluated. The net mesh size (0.3 mm for this study) is a variable to be taken into account (Michida et al. 2019; Tokai et al. 2021). At the time of the sampling campaigns, this mesh size was one of the most used for the recovery of microplastics from the sea surface (see, for example Moore et al. 2001; Hidalgo-Ruz et al. 2012), and it was considered the most suitable for the Northern Adriatic Sea average conditions. In particular, it represented a good compromise between the microparticles recovery efficiency and net clogging issues due to the frequent presence of floating biogenic materials (Michida et al. 2019). The potential underestimation of the SMP fraction, associated to the utilization of a 0.3 mm mesh size, is still an open issue, as suggested in Tokai et al. 2021, showing that particles smaller than 0.5 mm could not be sampled. However, during both sampling campaigns, a certain number of particles ranging from 0.3 to 0.475 mm was identified (Fig. 2S). On the other hand, in Botterell et al. (2019), reviewing literature data about bioavailability and effects of microplastics in marine zooplankton, the importance of investigating the finest fraction, with dimensions lower than 100 µm, which are expected to exhibit the greatest impact on biological organisms, was also highlighted.

Polymeric composition, category and colours

The polymeric composition of collected particles was determined by means of three different spectroscopic techniques in order to obtain a cross-confirmation of recognized materials. This multi-analytical approach also allowed to strongly reduce the number of unidentified items, compensating the intrinsic limits of each analytical method.

Results on MeP and LMP were mainly obtained by NIR spectroscopy, which identified the polymeric composition of 87% of analysed items, while a further 3% was recognized by using Raman spectroscopy. The chemical composition of 95% items in the 0.3–1 mm size range (SMP) was identified by combining Raman and FTIR-ATR spectroscopy: 57% was recognized when applying both analytical techniques, whereas 27% and 11% were determined exclusively by FTIR-ATR and Raman spectroscopy, respectively.

Table 2 reports the results (as percentage values) of polymer identification for each category (defined in the "Sample treatment, meso-/microplastic determination, particle image analysis and shape and size measurement" section), with SMP (the most relevant fraction) relative amounts in brackets.

Polyethylene (PE) was the most represented polymer, contributing to 39 and 66% of M1 and M2 samples, respectively, followed by polypropylene (PP, 21–22%). Polyvinylchloride (PVC) and polystyrene (PS) were found to contribute to a lesser extent. In total, polyolefins represented 59 and 88% of plastic particles collected in M1 and M2, respectively, while other polymers contributed 27.4% in M1 and 7.9% in M2.

As concerning the unidentified fractions, they represented the 13.6 and 4.1% of particles from M1 and M2, respectively. In most cases, their very dark colour and/or degradation impaired their spectroscopic identification.

As shown in Table 2, samples from M1 exhibited a greater variety in terms of polymeric composition, while in M2, the polyolefin fraction largely dominated the plastic debris mixture. In the M1 campaign, polyolefins represented 59.4% of all recovered particles and 34.8% of the finest fraction (SMP); parallel, in the M2 sampling, PE + PP were 88% of collected plastic debris (62.8% of SMP fraction). The PE/PP ratios calculated on the whole amounts of collected particles were 1.9 (M1) and 3 (M2), respectively, confirming the relevant prevalence of PE on PP, especially in the M2 session. Interestingly, in M1 the foam contribution represented more than 1/3 of overall PP particles.

Through the ratio values of (PE + PP)/OP (other polymers, i.e. PS, PET and PVC), two categories of plastics, whose density is lower (PE + PP) or higher (Other Polymers) than the seawater (1.027 g cm^{-3}), could be compared (foams, whose buoyant properties are not related to the polymer specific gravity but mainly to gases entrapped in the polymeric structure, were omitted). The obtained values of 2.5 and 12.5 for M1 and M2, respectively, indicated that polymers with higher density strongly increased the heterogeneity of the M1 composition. The potential contribution of unidentified (N.I.) items, potentially belonging to both groups, was also taken into account, identifying percentage ranges of 1.6–3.1 (M1) and 8.5–13.5 (M2), depending on whether N.I. were considered polyolefins or other polymers.

The comparison between the polymer percentage values obtained for M1 and M2 highlighted the largest contribution of "heavy" (i.e. more dense than seawater) polymers in the October campaign; this result can be explained in terms of different meteo-oceanographic conditions during sampling

Table 2 Percentage distributions of polymeric composition of recovered particles grouped in shape categories. SMP relative percentage amounts are reported in italic and brackets. Bold= ∑

% 0.3–10 mm (% *SMP*)		PE	PP	PS	PET	PVC	EVA	PUR	POM	N.I	∑ Category
Fragment	M1	30.0 (*16.3*)	9.8 (*8.7*)	3.3 (*3.3*)	1.1 (*1.1*)	13.1 (*11.9*)		1.1 (*1.1*)		9.9 (*7.6*)	**68.3 (*49.9*)**
	M2	57.5 (*44.1*)	15.9 (*12.3*)	1.9 (*1.6*)	0.3 (-)	2.7 (*1.6*)	0.3 (*0.3*)	0.3 (*0.3*)		2.7 (*1.6*)	**81.7 (*62.2*)**
Pellet	M1										
	M2			0.5 (*0.5*)							**0.5 (*0.5*)**
Granule	M1	1.1 (*1.1*)									**1.1 (*1.1*)**
	M2	1.9 (*1.9*)	0.5 (*0.5*)			0.3 (*0.3*)					**2.7 (*2.7*)**
Filament	M1		1.1 (*1.1*)							1.1 (-)	**2.2 (*1.1*)**
	M2	0.5 (-)	0.3 (-)							0.3 (*0.3*)	**1.1** (0.3)
Film	M1	7.5 (-)	2.3 (-)	1.1 (-)					1.1 (-)	1.1 (*1.1*)	**13.2 (*1.1*)**
	M2	5.7 (*1.6*)	5.2 (*1.6*)			0.8 (*0.8*)				0.3 (-)	**12 (*4.1*)**
Foam	M1		7.6 (*7.6*)	3.3 (*2.2*)		3.3 (*3.3*)				1.1 (*1.1*)	**15.2 (*14.2*)**
	M2		0.3 (*0.3*)	0.3 (-)	0.3 (*0.3*)	0.3 (*0.3*)				0.8 (*0.8*)	**1.9 (*1.6*)**
∑ Polymer	**M1**	**38.6 (*17.4*)**	**20.8 (*17.4*)**	**7.7 (*5.4*)**	**1.1 (*1.1*)**	**16.3 (*15.2*)**		**1.1 (*1.1*)**	**1.1** (-)	**13.2 (*9.8*)**	**100 (*67.3*)**
	M2	**65.8 (*48.0*)**	**22.2 (*14.8*)**	**2.7 (*2.2*)**	**0.5 (*0.3*)**	**4.1 (*3.0*)**	**0.3 (*0.3*)**	**0.3 (*0.3*)**		**4.1** (2.7)	**100 (*71.6*)**

(see the "Evaluation of the sampling conditions" section): higher wind speed in October increased mixing processes. In particular, plastic particles sunk on the seabed have been partially re-suspended within the water column.

Figure 6 shows the distribution of particles in terms of both composition and dimensional class along the two transects. It was not possible to detect any clear trend in the modification of particles sampled along M2, while the greatest percentage variability along M1 was displayed by PVC, except in tow M1.5 (5th of the transect). This result did not allow for individuating any relationship between the compositional change of this sample and the distance from the closest lagoon inlet (Malamocco).

When considering the composition of collected plastic debris in terms of categories, *fragments* constituted the most relevant part, with ~ 68% in M1 and ~ 82% in M2, especially for SMP (~ 50 and ~ 62% of all recovered plastic particles, respectively). As shown in Table 2, PE was the most represented polymer among fragments in both M1 (30%) and M2 (57.5%) in M2, while PVC and PP represented together the second most diffuse chemical group (13% and 16% in M1 and M2, respectively). Furthermore, *foams* and *films* were collected in relatively high percentages: 15% in M1 and 13% in M2, respectively. *Pellets*, *granules* and *filaments* were instead minor components of overall samples in both campaigns. In particular, the relative amount of *foams* was found to be higher in M1 than in M2, with the highest concentration measured in M1.1, being this the closest tow to the coast (Fig. 3S). This can be attributed to October relative windier weather conditions, allowing for a more effective recovery of lighter materials deposited along the shoreline by sea weaves.

As concerning the chromatic appearance ("Sample treatment, meso-/microplastic determination, particle image

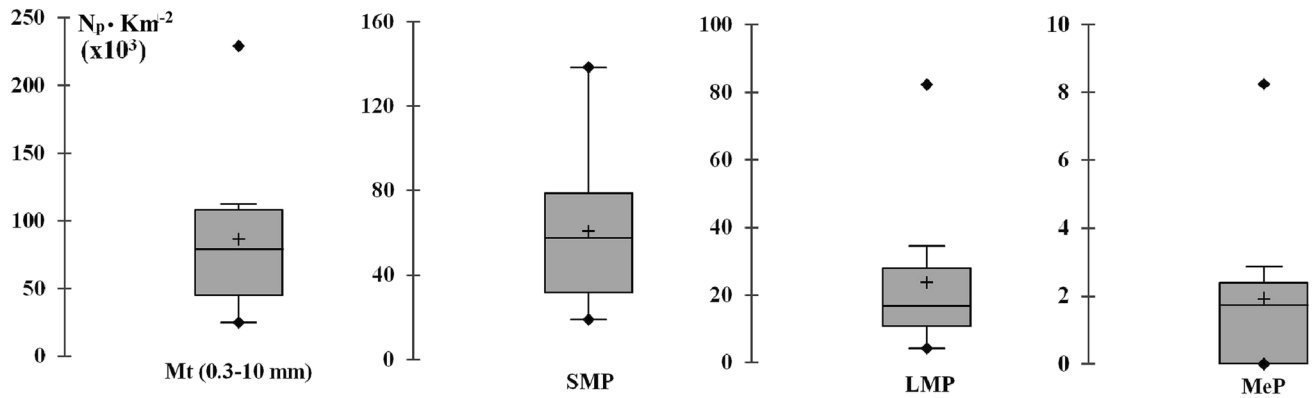

Fig. 5 Box plots of overall average Mt values for the whole particles size range (0.3–10 mm) and for each size class (SMP, LMP and MeP)[2 columns]

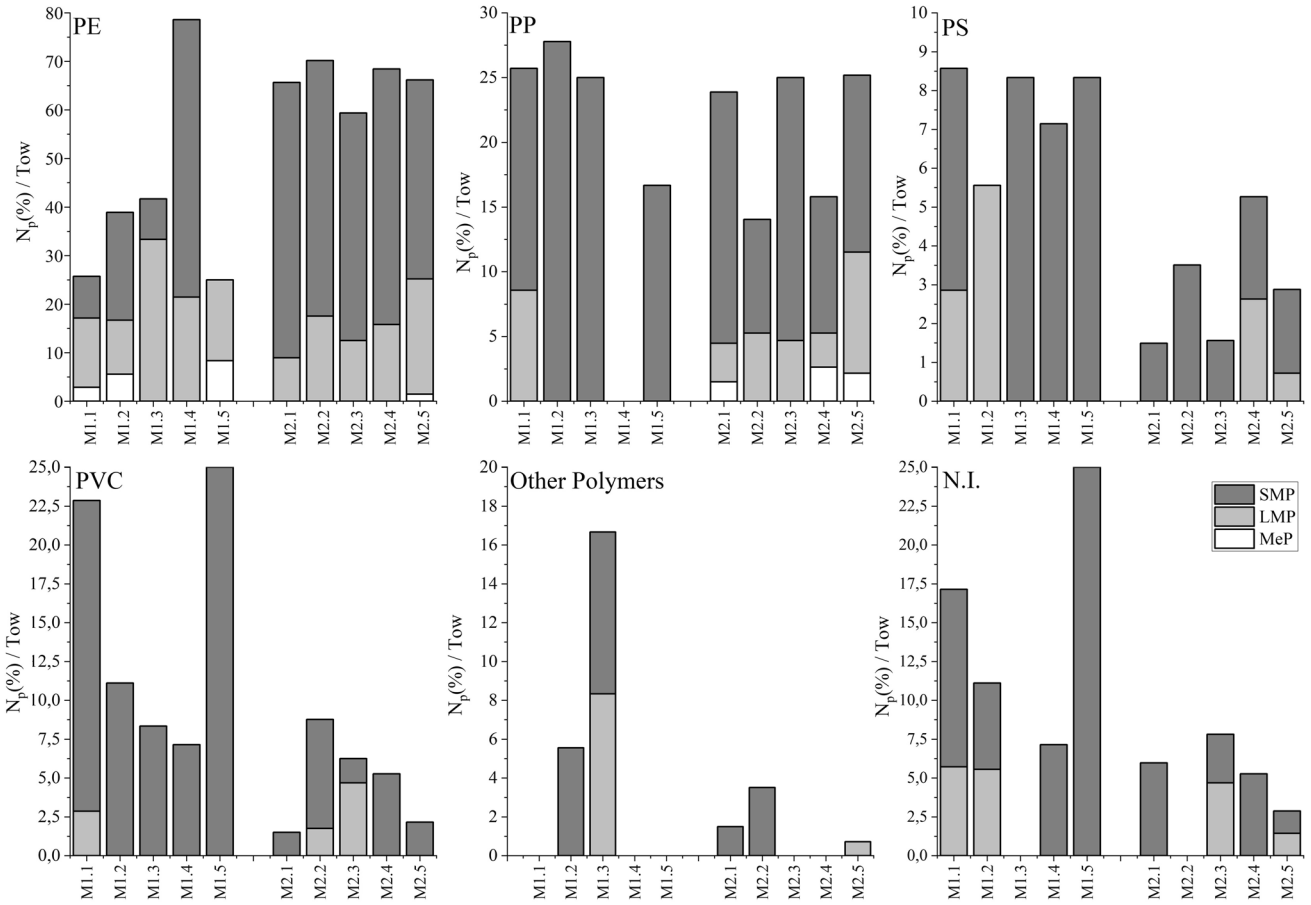

Fig. 6 Percentage distribution in terms of both polymeric composition and dimensional class (MeP, LMP, SMP) of collected particles along the sampled tows during M1 and M2

analysis and shape and size measurement" section), most of the collected plastic debris exhibited *white* and *clear-white-cream* (Hanke et al., 2013) hue colour (Table 3). Approximately, 62% and 44% of collected plastic particles showed a *white* colour in M1 and M2, respectively, while in this last sampling campaign, a *clear-white-cream* hue was identified in 32.6% of particles, probably originated by yellowing processes of white plastic polymers. Their prevalence can result from the contemporary abundance of light-coloured items, very close to native virgin pellets, and from leaching/degradation of plastics pigments and coloured coatings. This consideration is supported by the relatively small contributions found by other colours (except black and grey, see below) being 11 (M1) and 9% (M2) of recovered plastic particles. These results suggest them to be originated from plastic litter subjected to a prolonged stay in the seawater and to the simultaneous effects of sunlight, mechanical breakage, etc. (Singh and Sharma 2008; Andrady 2015, 2017; Martí et al. 2017; ter Halle et al. 2017).

Black and grey hues covered percentage amounts of 7.7 (M1)–12% (M2) and 6.3 (M1)–8.7% (M2), respectively. As already reported, this fraction included most of the particles unidentified in terms of chemical composition due to prevailing absorption phenomena.

As described in the "Sample treatment, meso-/microplastic determination, particle image analysis and shape and size measurement" section, the definition of classification of visual aspects such as *opaque*, *semi-translucent*, *translucent* or *transparent* was obtained through a customized procedure (Table 3). Opaque particles dominated in both M1 and M2 (57 and 41% in M1 and M2, respectively) with white opaque items being the most common. The lowest percentage values came from transparent particles (6.8–13.1), while those with intermediate optical properties, such as the translucent and semi-translucent ones, amounted to 36% and 45.4% in M1 and M2, respectively.

The results obtained on the compositional, category and colour analysis seem to indicate that most of the recovered particles originate from quite old floating items, remained in the sea environment for a relatively long time, and probably employed as packaging materials for food and/or other typologies of commercial goods.

Table 3 Percentage distribution of colours (Hanke et al., 2013) and optical properties of recovered particles. SMP relative percentage amounts are in brackets. Bold=∑

% 0.3–10 mm (*% SMP*)		White	Clear-white-cream	Yellow	Red	Tan	Brown	Blue	Green	Grey	Black	∑ Optical property
Opaque	M1	34.4 (20.6)	2.2 (1.1)		1.1 (1.1)	1.1 (1.1)			1.1 (1.1)	7.7 (6.5)	9.8 (9.8)	57.3 (*41.3*)
	M2	16.2 (*11.0*)	6.6 (5.5)	1.6 (*1.4*)	0.5 (*0.5*)	0.8 (*0.8*)	0.3 (*0.3*)	1.1 (*0.5*)	1.4 (*0.8*)	5.2 (*4.1*)	7.7 (5.5)	**41.4 (*30.4*)**
Semi-translucent	M1	10.7 (4.3)	2.2 (2.2)					1.1 (-)		1.1 (*1.1*)	1.1 (*1.1*)	**16.2** (8.7)
	M2	6.9 (5.5)	9.9 (8.5)	0.8 (*0.8*)		0.3 (-)			0.3 (*0.3*)	0.5 (*0.5*)		**18.6** (15.6)
Translucent	M1	11.0 (7.6)	1.1 (-)	6.5 (6.5)							1.1 (*1.1*)	**19.8** (15.2)
	M2	10.1 (*7.1*)	14.5 (*10.1*)	0.3 (-)				0.8 (*0.3*)	0.5 (*0.5*)	0.5 (*0.3*)		**26.8** (18.4)
Transparent	M1	5.6 (2.2)	1.1 (-)									**6.8** (2.2)
	M2	11.2 (5.5)	1.6 (*1.4*)			0.3 (*0.3*)						**13.1** (*7.1*)
∑ Colour	**M1**	**61.7 (*34.7*)**	**6.7** (3.3)	**6.5 (*6.5*)**	**1.1 (*1.1*)**	**1.1 (1.1)**		**1.1** (-)	**1.1** (1.1)	**8.7 (*7.6*)**	**12.0 (*12.0*)**	**100 (*67.3*)**
	M2	**44.4 (*29.1*)**	**32.6 (*25.5*)**	**2.7 (*2.2*)**	**0.5 (*0.5*)**	**1.4 (*1.1*)**	**0.3 (*0.3*)**	**1.9 (*0.8*)**	**2.2 (*1.6*)**	**6.3 (*4.9*)**	**7.7 (5.5)**	**100 (*71.6*)**

Creation of the specific groups

In order to compare the results of the two sampling campaigns, diversity indexes were used by applying categories, i.e. specific groups (*sg*), in turn obtained by gathering the particles properties. The full characterization of each particle (dimension, composition, shape category, colour, optical properties) data are in fact difficult to handle and interpret when huge quantities of particles are collected.

All obtained data previously discussed were applied to define the sgs as reported in Sect. 2.7. Table 4 reports the distributions of plastic particles in sgs both as absolute abundance ($\sum sg_i$) and as relative frequency ($\sum sg_i/SG$ (%)). Also the corresponding number of particles, both as absolute abundance ($\sum n_i$) and as relative frequency ($\sum n_i/N_p$(%)), has been reported for each sampling campaign.

A total of 3656 sgs was generated, but only 50 and 95 of them were individuated exclusively in M1 or M2; 32 sgs resulted to be common to both sampling campaigns (M1 ∩ M2) and represented 64% of M1 and 34% of M2 (Table 4).

When considering the relative abundance of particles associated to a specific sg (Table 4), data of common sg ($\sum n_i/N_{p.}$ (%) value for M1 ∩ M2) that correspond to 68% and of 57% were reached for the two sampling campaigns, respectively.

Furthermore, the relative frequencies (f) of particles belonging to each sg were calculated in relation to the total amounts of the recovered ones in M1 and M2. The sgs in common for M1 and M2 were clustered in seven classes on the basis of their relative amounts of particles: (i) $f > 10\%$, (ii) $8\% < f \leq 10\%$, (iii) $6\% < f \leq 8\%$, (iv) $4\% < f \leq 6\%$, (v) $2\% < f \leq 4\%$, (vi) $1\% < f \leq 2\%$ and (vii) $f \leq 1\%$ (Table 5; the composition of the first 5 frequency classes is reported in Table 3S). The comparative distribution of particle abundances in relationship to sg classes ($\sum f > n_i/N_{p.}$ %) is given in Fig. 7. The numbers indicate the cumulative amounts of sgs in each class (black scale) and the cumulative percentage amounts of plastic debris for all classes (red scale), while histograms display the inverse cumulative distributions of overall data, related to particle numerosities for M1and M2 and reported as percentage; red dotted areas refer to the M1 ∩ M2 subset data. The black line and circles represent data related to number of sgs; black dotted lines and grey circles refer to the M1 ∩ M2 subset data. Figure 7 (supported by data in Table 5) allows giving a descriptive overview of the sample features (e.g. their composition in terms of microplastics typologies) each of them consisting in a specific combination of features.

For M1, microplastics resulted to be mainly associated with sgs exhibiting numerosity frequency between 1 and 4%, including 68% of collected particles distributed in 45 of the 50 total sgs (90%). On the other hand, when referring to the

Table 4 Number of sgs ($\sum sg_i$) and corresponding number of particles ($\sum n_i$), relative frequency of sg ($\sum sg_i/SG$ (%)) and of the corresponding relative abundance of particles ($\sum n_i/N_p$ (%)) for M1 and M2. M1 ∩ M2 = values for sgs in common to both campaigns; Mx-(M1 ∩ M2) = values for sgs not in common to M1 and M2

	$\sum sg_i$		$\sum n_i$		$\sum sg_i/SG$ (%)		$\sum n_i/N_p$ (%)	
	M1	M2	M1	M2	M1	M2	M1	M2
	50	95	91	365				
M1 ∩ M2	32	32	62	208	64	34	68	57
Mx-(M1 ∩ M2)	18	63	29	157	36	66	32	43

Table 5 Distribution of particles, as number ($\sum n_i$) or percentage ($\sum n_i/N_p$) for frequency classes (*f*) by grouping as sg ($\sum sg_i$). Data reported in square bracket are related to common sgs (M1 ∩ M2). Bold= $\sum$

	M1			M2		
	$\sum sg_i$	$\sum n_i/N_p$	$\sum n_i$	$\sum sg_i$	$\sum n_i/N_p$	$\sum n_i$
	n	%	n	n	%	n
f **> 10**	1 [1]	13 [13]	12 [12]	1 [-]	11 [-]	40 [-]
8 < ***f*** **≤ 10**				1 [1]	10 [9]	35 [35]
6 < ***f*** **≤ 8**				2 [1]	13 [6]	47 [25]
4 < ***f*** **≤ 6**	4 [3]	19 [13]	17 [12]	3 [3]	15 [14]	54 [53]
2 < f ≤ 4	13 [8]	33 [20]	30 [18]	4 [4]	12 [11]	43 [43]
1 < f ≤ 2	32 [20]	35 [22]	32 [20]	9 [3]	13 [5]	48 [19]
f **≤ 1**				75 [20]	27 [8]	98 [32]
∑	**50 [32]**	**100 [68]**	**91 [62]**	**95 [32]**	**100 [56]**	**365 [208]**

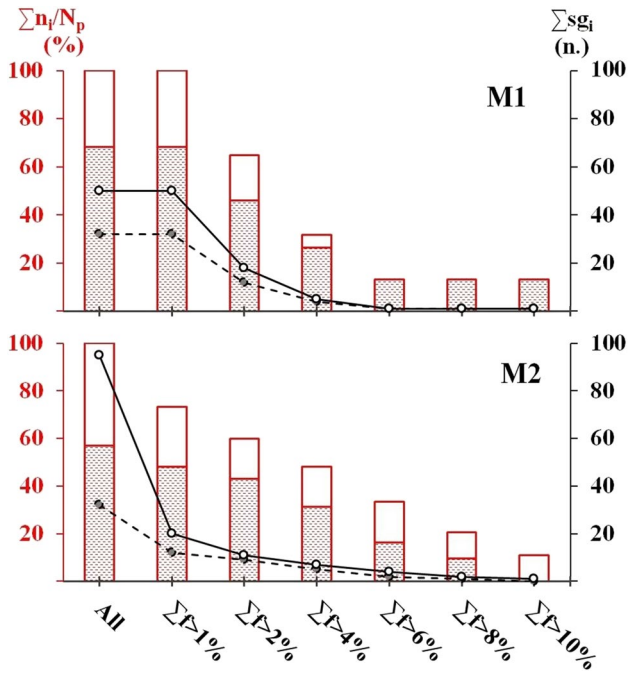

Fig. 7 Comparison of the inverse cumulative distribution of particles ($\sum n_i/N_p$ as %, red histogram and red scale on the left) associated to specific groups ($\sum$sgi, expressed as number, black hollow point/solid line and black scale on the right) in relationship to the increase of cumulative frequency classes for the sampling campaign M1 and M2. Data related to common specific group (M1 ∩ M2) are reported in dotted red part of histograms and grey point/black dashed line

same numerosity frequencies (1–4%), a total of 88 sgs was obtained for M2, representing 93% of the sgs in M2 (95 in total) and covering 52% of identified particles.

The absence of sgs with $f < 1$ in M1 was evident, whereas the sgs with $f > 10$ are approx. 2% (1 sg on 50 containing 13.2% of particles for M1). In M2, conversely, most of the sgs presented low frequencies of microplastic particles: 75 sgs on 95 (79%) were related to $f \leq 1$ frequency class, contributing to only 27% of total plastic particles. In M2, particles falling in the classes with $f > 1$ distribute in the remaining 20 *sgs*, each of them including approximately 10–15% of collected microplastics and totally representing the 73% of collected particles. In particular, single sg covers the $f > 10$ class, consisting in 11% of the total amount of collected particles.

Furthermore, the common sgs (M1 ∩ M2) fell, mainly, in the frequency class $f \leq 2$: 20 and 23 out of 32 in M1 and M2, respectively; they represent the 62.5% (M1) and 72% (M2) of the common sgs and the 22% and 13% of collected particles for M1 and M2, respectively.

The results of Shannon (*H'*) and Simpson Indexes (D_s) for both monitoring campaigns are shown in Table 6. The reported data pointed out that M1 and M2 floating plastics resulted well diversified in terms of *sgs* presence, and they were uniformly distributed within them. This is due to the fact that plastic particles probably originated from different sources and processes, as also suggested by the trends identified in Fig. 7,

Table 6 Shannon (H' H'^{max}, $E_{H'}$ evidenced in grey) and the Simpson Index ($D_{s,}^{max}$, $E_{Ds,}$) values obtained for M1 and M2

	H'	H'^{max}	$E_{H'}$	D_s	D_s^{max}	E_{Ds}
M1	3.630 (±0.103)	3.912	0.928 (±0.026)	0.972 (±0.009)	0.980	0.992 (±0.009)
M2	3.722 (±0.069)	4.554	0.817 (±0.015)	0.959 (±0.004)	0.989	0.969 (±0.004)

indicating that a huge number of sg_is exists, each accounting for very low percentages of particles.

Based on a two-tail t-test, with a t-value = 0.74 and considering a reference value of $t_{183} = 1.653$ for $\alpha = 0.05$, it is not possible to reject the hypothesis that the H' values for M1 and M2 are equivalents. At the same way, for the two-tail t-test D_s, with a resulting t-value = 1.39, and considering a reference value of $t_{454} = 1.648$ for $\alpha = 0.05$, it is not possible to reject also the hypothesis that D_s values calculated for M1 and M2 are equivalent. The analysis of these two diversity indexes pointed out that micro- and mesoplastic items set structures deriving from both M1 and M2 campaigns do not differ significantly. However, $E_{H'}$ values for data reported in Table 6 seem to indicate that a lower level of evenness exists for M2 than for M1. This is probably due to the fact that M2 accounted for a higher number of sgs, each of them including a greater number of particles (Fig. 7). In parallel, also E_{Ds} values for M1 resulted higher than those obtained for M2.

The proposed approach, based on the generation of sgs, allowed managing a relevant amount of data related to various aspects of the collected particles, such as colour, shape, optical properties and composition. This allowed, in turn, evaluating the heterogeneity level within each sampling campaign, as well as the diversity and the evenness degrees between M1 and M2. The obtained data were elaborated through a graphical approach in order to display the particles' abundance distribution related to all the sg_is. Moreover, a qualitative assessment of the diversity in the sg_is assemblages between the two samples' sets (M1 and M2) was also performed in order to detect richness, prevalence or any other sorting trends among sg_is. This approach was finalized in order to identify potential quantitative tools aimed to individuate source and generation processes of plastic debris in the marine environment.

Oceanographic conditions and comparison with literature data

Currents and circulation in the Northern Adriatic Sea

The northern part of the Adriatic Sea is the most extensive shallow water area in the Mediterranean Sea (Buljan and Zore-Armanda 1976; Zavatarelli et al. 2000; McKinney 2007a) with a mean depth of 35 m, accounting only for about 5% of the total water volume of the Adriatic Sea, (Buljan and Zore-Armanda 1976). Despite this, it contributes with relevant amounts of riverine water to the overall water budget of the basin. Approximately, 25% of overall riverine waters is discharged by the Po river, while a further 40% deriving by other rivers (such as Adige and Tagliamento) located between the Po and Isonzo mouths (Raicich 1994; McKinney 2007a). This water inflow is deviated southward along the Italian coast by the Coriolis effect and drives together with an entering seawater flow from the Ionian Sea, a baroclinic cyclonic surface circulation (Artegiani et al. 1997; Poulain 1999, 2001). It has a counterclockwise flow at Adriatic basin-wide scale southward along the Italian coast and northward along the eastern side. The coastal configuration and conformation of seabed split the overall flow into three smaller cyclonic gyres (McKinney 2007b). While the cyclonic gyres in the southern and central parts of Adriatic basin exhibit a quite constant presence throughout the year (Zorè 1956; Rizzoli and Bergamasco 1983), the northern one is more affected by seasonal trends and larger variability. Its presence is limited to the autumn–winter period (Artegiani et al. 1997), and in this shallow section of the Adriatic Sea, the largest intensity variations of surface currents (McKinney 2007b) can be experienced in late fall-winter. The Northern Adriatic Sea in this period behaves as an open basin with a strong water circulation and exchange with the other Adriatic sub-basins (Mosetti and Lavenia 1969; Zore-Armanda and Gačić 1987), while in the spring and the summer seasons, it exhibits a reduced interchange of its low density water mass with the southern section, thus acting as a semi-closed basin (Krajcar 2003; McKinney 2007b, 2007c). In the fall-winter season, a further cyclonic gyre can be generated by wind-driven circulation in this area which presence and position are strongly dependent on the presence and intensity of the Bora wind, blowing from E/NE toward Italian coasts. At the same time, a weak anticyclonic gyre (interposed between this one and those examined above) accordingly is generated (Zore-Armanda and Gačić 1987; Orlić et al. 1994; Mauri and Poulain 2001). Bora is the prevailing wind in the North Adriatic (Cavaleri et al. 1997) during the cold seasons, but it does not act constantly

in time. It accumulates water onto the Italian coast (Bergamasco and Gačić 1996), enhancing a baroclinic coastal flow, due to the water discharge from the northern Italian rivers (Kourafalou 2001), and generating a lower salinity southward current flowing strictly along the Italian coast (Orlić 1989). However, the described winter circulation gyres are ephemeral meteo-oceanographic structures.

The general circulation in the Northern Adriatic Sea is due to various forcing elements interacting for its establishment, such as the water density and the windshear, which can interact with each other, deeply varying between seasons and from year to year (McKinney 2007b).

The impact of such seasonal circulation dynamics on plastic litter distribution in the Adriatic Sea has been studied by Liubartseva et al. in 2016, proposing a debris transport model at regional scale in the frame of a wider study on the plastic debris presence in the basin. It was pointed out that areas with the highest concentrations of plastic debris represent an elongated band disposed toward and along the Italian coast. It displays a progressive narrowing from northwest (covering an area between the Po Delta and the Gulf of Trieste) to southeast. This would mean that debris distributes mainly according to seasonal circulation dynamics previously discussed and that areas with high plastic litter concentrations can be individuated in both the northern part of the Adriatic Sea and along the entire Italian coastline.

At local scale, the surface currents in front of the Venice Lagoon, i.e. the southward thermohaline circulation near the lagoon inlets, interact also with the tidal flow through them. In front of the Malamocco lagoon inlet, close to the sampling sites, two counter-rotating mini vortices of about 4–5 km each usually insist, except during the Bora wind blowing (Gačić et al. 2009). This suggests that also local and sub-mesoscale processes impact microplastics distribution in this area. Both sampling campaigns were carried out during the fall season; therefore, the concentration of microplastics can be affected mainly by surface water circulation, characterized by a general southward water flow and by the interaction of surface water with the shallow sea bottom. This is due to potential mixing conditions occurring in the water column, including a loss of the vertical stratification, which would be very likely due to the weather and sea constraints typical of the fall season.

The complex situation described above needs to be carefully taken into consideration for the correct interpretation of results obtained in this study and for a comparison with data reported in the literature related to other Adriatic or Mediterranean areas.

Indeed, differences in both amounts and typologies of micro-plastics collected in M1 and M2 can be due to transport phenomena along the coast driven by the cyclonic circulation. For example, samples collected in both M1 and M2, carried out close to the coastline, displayed huge amounts of weathered materials, as shown by the prevalence of whitish-yellowish colours (Martí et al. 2020). However, some differences were found with respect to what is reported by Martí et al. (2020), reporting the highest amounts of degraded plastic particles as collected far from the costs. Consequently, it is possible that the weathering of plastic materials, collected in this study close to the shoreline, occurred during the long time they spent in the coastal cyclonic circulation.

Comparison with literature data

As reported by Zhang (2017), seasonal evolutions caused by gyres or other meteo-oceanographic phenomena (see the "Currents and circulation in the Northern Adriatic Sea" section) affect microplastic transport and accumulation among coastal seas. A comparison of results obtained in this work with literature about the Mediterranean Sea is reported in Table 7 and Fig. 8, together with a selection of literature data focused on other coastal, semi-enclosed or enclosed seas (Healy and Harada 1991).

Authors reported data either as $N_p \bullet km^{-2}$ (Table 7a and Fig. 8) or as $N_p \bullet m^{-3}$ (Table 7b and Fig. 8); values related to the present study were plotted as well in order to simplify the comparison.

The investigation by Vianello et al. (2018) reported about data collected for two transects in areas close to the ones investigated in this study. The authors moved from coastline to deep sea located southernmost, in front of Pellestrina Island (a barrier island of Venice Lagoon) and of Po River delta (Vianello et al. 2018). The sampling sessions were performed in March and April 2014, and the microplastic concentrations (mean overall data in Table 7 and Fig. 8) were reported as $N_p \bullet km^{-2}$, falling in the ranges $(1–104) \cdot 10^5$ (March 2014) and $(13) \bullet 10^5$ (April 2014) for the Pellestrina Island. In parallel, data for the Po Delta transect showed ranges within $(2–43) \bullet 10^5$ and $(0.3–6) \bullet 10^5$ for both periods, respectively (Vianello et al. 2018). Data acquired near Pellestrina are comparable with those obtained in this work in terms of concentration of microplastics longshore ($(0.2–2.3) \bullet 10^5$ $N_p \bullet km^{-2}$), excluding the "hot spot" ($10.4 \bullet 10^6$) that Vianello et al. detected at the seaward station. The high plastic micro-litter accumulation in this "hot spot" was considered by the authors as due to the passive transport driven by cyclonic circulation of the basin.

Other data available for this Adriatic area were reported for the Gulf of Trieste along the northern Istrian Coast from monitoring campaigns carried out between 2012 and 2014. Data, ranging from $0.01 \bullet 10^6$ to $3.1 \bullet 10^6$ $N_p \bullet km^{-2}$ (Gajšt et al. 2016), confirmed the values obtained for the Veneto coast, with a microplastic contamination level between 10^4 and 10^7 $N_p \bullet km^{-2}$. Such values are in good agreement with the average concentration of $3.15 \bullet 10^5$calculated for the Gulf of Split (Croatia), the Gulf of Trieste (Slovenia), Cesenatico (Emilia

Table 7 Comparison of data from literature on enclosed, semi-enclosed and coastal areas. Data shown as reported by the authors. Bold = average value; [] = standard deviation

Site	Year of sampling	n•10^5/km^2		Size range	Sampling method	Mesh	Ref
		Average value	**Min.–max**				
NW. Adriatic Sea: Veneto Coast, Italy	2015	**0.87**	0.25–2.29				**Present study**
NW. Mediterranean Sea: Ligurian S.- Corsica- Elba- G. of Lion	2010	**1.16**	0–8.92	mP	Manta net	333	Collignon et al. (2012)
NW. Mediterranean Sea: Corsica, Bay of Calvi	2010	**0.17** [0.44]	0–2.17	SmP	Necton net	200	Collignon et al. (2014)
		0.35 [0.83]	0–3.95	LmP			
W. Mediterranean: G. of Lion-Balearic Is.-Corsica-Sardinia	2011–2012	**1.30**	0.10–4.20	mP	Manta net	333	Faure et al. (2015)
Across Mediterranean Sea Basin	2013	**2.44**		mP/Mep/MaP	Neuston net	200	Cózar et al. (2015)
NW. Mediterranean: Ligurian Sea	2013		0.21–5.78	mP/MeP	Manta net	333	Pedrotti et al. (2016)
Mediterranean subbasins	2011–2013	**1.47 [**0.25]	0.09–11.60	mP/Mep/MaP	Manta net	333	Ruiz-Orejón et al. (2016)
Sardinian Sea	2011–2013		0.09–3.30	mP/Mep/MaP			
Tyrrhenian Sea	2011–2013		0.11–6.17	mP/Mep/MaP			
Ionian Sea	2011–2013		0.16–11.60	mP/Mep/MaP			
Adriatic Sea	2011		0.14–9.82	mP/Mep/MaP			
Mediterranean subbasins	2013	**12.50**	0.40–92.30	mP/Mep	Neuston net	200	Suaria et al. (2016)
S. Adriatic- N. Ionian Sea	2013		0.40–46.50	mP/Mep			
S. Tyrrhenian—Sicily Strait—Algerian Basin	2013		1.10–24.00	mP/Mep			
Ligurian Sea, N. Corsica	2013		3.40–92.30	mP/Mep			
Sardinian Sea	2013		7.70–69.00	mP/Mep			
N. Adriatic Sea: Slovenian Coast	2012–2014	**4.72** [8.28]	0.14–30.98	mP/Mep	Manta net	300	Gajšt et al. (2016)
Adriatic Sea	2014–2015	**3.15**		mP/Mep	Manta net	330	Zeri et al. (2018)
NW. Mediterranean: Ligurian-N. Tyrrhenian Sea	2014	**0.82** [0.79]		mP	Manta net	330	Fossi et al. (2017)
NW. Adriatic Sea: Pellestrina Island (Veneto Coast, Italy)	2014	**14.4**	1–104	mP	Manta net	330	Vianello et al. (2018)
NW. Adriatic Sea: Po River Delta (Veneto Coast, Italy)		**9.79**	0.3–43				
E. Mediterranean: NE. Levantine Turkish Coast	2016	**3.76**		mP/Mep	Manta net	333	Gündoğdu and Çevik (2017)
Marmara Sea	2017	**12.63** [13.05]	0.90–32.00		Manta net	333	Tunçer et al. (2018)

Table 7 (continued)

Site	Year of sampling	n•10^5/km^2		Size range	Sampling method	Mesh	Ref
		Average value	**Min.–max**				
Baltic Sea: Stockholm area and Outer Archipelago	2014	**1.10** [1.51]	0.16–6.18	mP	Manta net	333	Gewert et al. (2017)
North Sea-Celtic Sea-English Channel	2011	**0.37** [0.46]	0.00–3.76	mP	Manta net	333	Maes et al. (2017)
Red Sea: Arabian Coast	2016–2017	**0.04** [0.08]	0–0.50	"fragments"	Manta net	150	Martí et al. (2017)
Persian Gulf: E. Qatar—Doha Bay	2015	**4.04**	0.44–14.60	mP	Neuston net	300	Abayomi et al. (2017)
NW. Atlantic Ocean: Chesapeake Bay	2011		0.06–2.98	mP	Manta net	330	Yonkos et al. (2014)
		n/m^3					
NW. Adriatic Sea: Venetian Coast	2015	**0.44**	0.13–1.17				Present study
NW. Mediterranean: Ligurian S.-Sardinia, G. of Asinara	2011	**0.62** [2.00]	0–9.67	mp	WP2 net	200	Fossi et al. (2012)
W. Mediterranean: Sardinia, G. of Oristano	2012–2013	**0.15**		mp	Manta net	500	de Lucia et al. (2014)
NW. Mediterranean: Sardinia- G. of Asinara	2012–2013	**0.16** [0.31]		mP	Neuston net	333	Fossi et al. (2016)
Ligurian Sea	2012–2014	**0.49** [1.66]		mP			
E. Mediterranean: Israeli Coast	2013–2015	**7.68** [2.38]	0.24–324.1	mP	Manta net	333	van der Hal et al. (2017)
NW. Mediterranean: G. of Lion-Rhône Estuary	2016	**0.18**	0.08–0.41	mP	Manta net	333	Constant et al. (2018)
Black Sea: S.E. Coastal Water	2014–2015	**1.1** [0.9] •**10^3**	160–3.28•10^3	mP	WP2 net	200	Aytan et al. (2016)
N. Baltic: Swedish coast	2007	**1.3** [0.8] •**10^3**		mP	WP2 net	90	Gorokhova (2015)
Baltic: Gulf of Finland	2013	**0.2** [0.2]	0–0.8	mP	Manta net	333	Setälä et al. (2016a)
S. Baltic: Bornholm Basin	1991–2015	**0.21** [0.15]	0.11–0.28	mP	Bongo net	150	Beer et al. (2018)
S. Baltic: S. Funen Archipelago	2015	**0.07** [0.02]	0.05–0.09	mp	Manta net	300	Tamminga et al. (2018)
S. North Sea: Jade estuary	2011	**6.4** [1.94] •**10^4**	0–1.77•10^6	mP	Bottle + filter	40	Dubaish and Liebezeit (2013)
English Channel: Tamar Estuary—Plymouth	2012	**0.03**		mP/MeP	Manta net	300	Sadri and Thompson (2014)
Persian Gulf: E. Qatar Coast	2015	**0.71**	0–3	mP	Conical net	120	Castillo et al. (2016)
East China Sea	2013	**0.17** [0.14]	0.03–0.46	mP	Manta net	500	Zhao et al. (2014)
Bohai Sea	2016	**0.33** [0.34]	0.01–1.23	mP	Manta net	330	Zhang et al. (2017)
Bohai Sea -Yellow sea- East China Sea	2016–2017		680–6.44•10^3	mP	Vacuum filtration	20	Qu et al. (2018)
Yellow Sea	2016	**0.33** [0.28]	0.12–0.51	mP	Manta net	333	Wang et al. (2018)

Table 7 (continued)

Site	Year of sampling	n•10^5/km^2		Size range	Sampling method	Mesh	Ref
		Average value	**Min.–max**				
Bohai Sea	2016	**2.2** [1.4] **•10^3**	400–5.2•10^3	mP	Bucket + filter	5	Dai et al. (2018)
N. Yellow Sea	2016	**545** [282]		mP	Niskin bottle + sieve	30	Zhu et al. (2018)
Seto Inland Sea (Japan)	2010–2012	**0.39**		mP	Neuston net	350	Isobe et al. (2014)
Sea of Japan-N. Pacific-Korea strait-East China Sea	2014	**3.74** [10.40]	0.03–491	mP	Neuston net	350	Isobe et al. (2015)
Korea Strait: Geoje Island	2012	**47** [192]	0.4–54.5*	mP	Manta net	330	Song et al. (2014)
E. Pacific Ocean: S. California, Santa Monica Bay	2001	**3.92**		mP/MeP	Manta net	333	Lattin et al. (2004)
Gulf of Mexico: Louisiana Shelf Water	2015	**11.10** [2.80]	0.2–18.4	mP	Neuston net		Di Mauro et al. (2017)

Romagna, Italy) and the Gulf of Corfù (Zeri et al. 2018). In these areas, manta sampling surveys were performed between 2014 and 2015, covering a large portion of coastal areas. Furthermore, in this last study, two maxima in microplastic concentrations (3.23•10^6 and 1.62•10^6 N_p•km^{-2}) were registered in the offshore waters of Cesenatico (April 2015) and Corfù Island (October 2014), respectively. Except for these two areas, significantly higher microplastic abundances in the nearshore water (≤ 4 km) were observed with respect to the offshore water (> 4 km) (Zeri et al. 2018).

Other studies covering additional Adriatic areas showed microplastics' amounts between 0.14•10^5 and 9.82•10^5 N_p•km^{-2} for the central and southern part of the Adriatic Sea, respectively (Ruiz-Orejón et al. 2016). In 2013 Suaria et al. focused on sampling sites mainly distributed along the Italian coast, reporting for a range of 0.40•10^5–46.50•10^5 N_p•km^{-2} in the area located between the South Adriatic and the North Ionian Sea, near to the Otranto Canal (Suaria et al. 2016). The authors used a manta net with a smaller mesh (0.2 mm) than that employed in the present study, which possibly affected the total amount of collected particles. Data reported by the authors showed also a higher abundance of microplastics with respect to what was found in this and other studies focused on the northern area of the Adriatic Sea.

Table 8 reports a summary of the particle polymeric compositions from some of the studies cited in Table 7 and Fig. 8 (only a limited number of these papers provided the information about the chemical compositions of microplastics). A comprehensive information about the percentage abundance of specific plastic polymers was reported in approximately 38% of the scientific articles here reviewed, mainly using FTIR spectroscopy, often in ATR configuration (33% of cases).

As previously reported (see the "Polymer identification" section), in this work, Raman spectroscopy has been associated with FTIR-ATR in order to allow a cross-validation of plastic materials, together with the use of NIR for the LMP. The limited number of items, less than one thousand, permitted the whole set of samples to be analysed. When huge numbers of items are collected, such as during extensive oceanographic cruises, it is not possible to analyse the whole sample, so a subsampling approach must be followed, often covering from 7 to 50% of the particles. A precise strategy was proposed by Vianello et al. (2018), where abundance of items steered the consistency of fraction subjected to analysis: 10% when at least 500 particles are collected, 50% when their number ranges from 500 to 100 and 100% for less than 100 particles. The results reported in the present study for the Malamocco Inlet area (Table 2, "Polymeric composition, category and colours" section) are in good agreement with data reported by other authors (Table 8), confirming the prevalence of PE and PP for the Adriatic area. In particular, a quite low percentage of PE-based particles (~ 39–66%) was detected with respect to other literature studies: amounts in the Mediterranean Sea have been estimated in the 52–78% range. Only Suaria et al. (2016) reported a contribution close to 40% for PE microparticles, resembling the ~ 39% found at the Malamocco Inlet. A PE percentage value very close to that detected at the Malamocco Inlet area was reported for the Tamar River mouth (South UK) (Sadri and Thompson 2014). Finally, data from the second campaign of this study (December 2015) were in good agreement with average data reported for Pellestrina Island (Vianello et al. 2018), a sampling site very close to the one here reported. The relative quantities of PE and PP-based particles amounted in that site to 60% and 22%, respectively, close to 66% for PE and

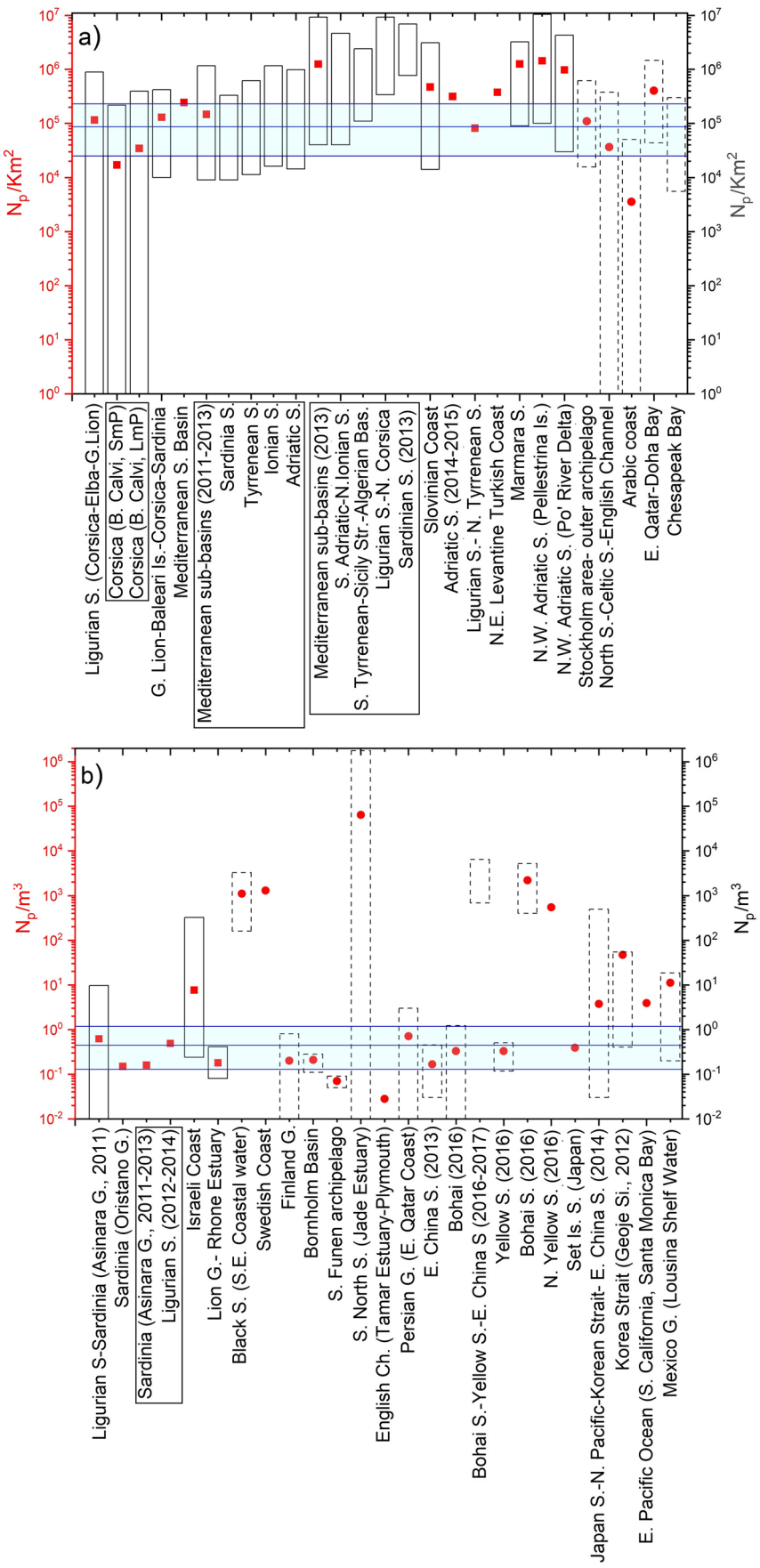

Fig. 8 Comparison of data from literature on enclosed, semi-enclosed and coastal areas. Columns, range of number of plastic particles (min–max values); red dots, average value; blue lines, max, average and min value of this study; black boxes, locations from the same study. **a** Mediterranean Sea and Extra Mediterranean Seas, number of particles per Km^2; **b** Mediterranean Sea and Extra Mediterranean Seas, number of particles per m^3

Table 8 Comparison of polymeric composition data from literature on enclosed, semi-enclosed and coastal areas. * = prevailing polymers, no data reported; ^ = original data corrected for cotton fibres contribution; § = ∑No Polyolefin. Data shown as reported by the authors

	Analysed materials	PE	PP	"Polyolefins"	PET/PES	PS	PVC	PA	ABS	Other polymer or ∑No polyolefins (§)	Unidentified polymer	
NW. Adriatic Sea: Veneto Coast, Italy	**mP/MeP**	38.6	20.8		1.1	7.7	16.3			2.2	13.2	Present study (Oct. 2015)
		65.8	22.2		0.5	2.7	4.1			0.6	4.1	Present study (Dec. 2015)
NW. Mediterranean: Ligurian Sea	**mP/MeP**	62–76	7–14							8–29	2	Pedrotti et al. (2016)
Mediterranean Sea Sub-basins	**> 700 µm**	52	16			2.8	2.6	4.7		21.9		Suaria et al. (2016)
N. Adriatic Sea: Slovenian Coast	**mP/MeP**	70	1.6	8.1		3	2		2	1.3	12	Gajšt et al. (2016)
Adriatic Sea		66.5	17.9		1	4.4		3		7.2		Zeri et al. (2018)
NW. Adriatic Sea: Veneto Coast, Italy	**mP**	60	22			4				14		Vianello et al. (2018)
NW. Mediterranean: Ligurian-N. Tyrrhenian Seas	**mP**	76.3	20.3			1.7				1.7		Fossi et al. (2017)
	MeP	78.6	2.4			19						
NW. Mediterranean: G. of Lion-Rhône Estuary	**fibres**		25^		47^			3^		25^		Constant et al. (2018)
	fragm./films	54	17							29§		
	foams					67				33		
Baltic Sea: Stockholm area and Outer Archipelago		53	24							23§		Gewert et al. (2017)
Tamar river estuary—Plymouth		40	19		6	25	7	3				Sadri and Thompson (2014)
Red Sea—Arabian Coast		69	21			4	3	1		2		Martì et al. (2017)
Persian Gulf: E. Qatar Coast		20	30			3.3		3.3	6.7	36.7		Castillo et al (2016)
Bohai Sea		51	29		3	16				1		Zhang et al. (2017)
Bohai Sea -Yellow Sea- East China Sea		3	2		74		3			17		Qu et al. (2018)
Yellow Sea		*			20					*		Wang et al. (2018)
N. Yellow Sea		77.8	11.1							11.1		Zhu et al. (2018)
Seto Inland Sea (Japan)	**mP**	68	19							13§		Isobe et al. (2014)
	MeP	53	25							22§		

22% for PP (Table 8) of this study. The relevant amount of PVC particles collected in the first campaign (16%) found confirmation only in data reported for the southern part of the Adriatic Sea (~ 8% of occurrence, data not reported in Table 8) (Suaria et al. 2016).

Conclusions

In recent years, many studies demonstrated the widespread contamination by microplastics of marine environment. This paper aimed to provide additional data on microplastics occurrence in the Northern Adriatic Sea. Two sampling campaigns were performed in October (M1) and December 2015 (M2) in the marine coastal area close to the Venice Lagoon (Italy) inlet.

Samples were characterized in detail by applying a multitechnique analytical approach involving three different spectroscopic methods, i.e. near infrared, FTIR-ATR and Raman spectroscopy in order to overcome analytical limits of each individual technique. This allowed an almost complete compositional screening of the plastic particles, supporting a reliable evaluation of their areal density ($N_p \cdot Km^{-2}$) in the studied area. The collected particles were also classified in terms of dimension, composition, categories, colour and other optical properties. The number of collected particles increased more than double in the time interval elapsed between M1 and M2 sampling sessions, with SMP providing the higher contribution (~ 67–72%), LMP ranging between 26.5 and 30% and MeP representing the smallest fraction (2–3%).

The spectroscopic analysis pointed out the larger contribution of polymers heavier than seawater in M1 than in M2, possibly due to the different meteo-oceanographic conditions during their sampling, such as a higher average wind speed in October. This can have favoured mixing processes leading to a re-suspension of plastic debris sunk on the seabed. This effect is particularly significant in the investigated Adriatic area, due to its shallow waters.

The collected plastic microplastics were also classified on the basis of the category: *Fragments* constituted the most relevant fraction (68–82%) with PE being the most represented polymer (30–57.5%), followed by PVC and PP. *Foams* and *films* were also found in quite high percentages (13–15%), while pellets, granules and filaments were minor debris components.

Concerning particles' colours and optical properties, most of them showed a *white* colour (62–44%) or a *clear-white-cream* hue (~7–33%), probably due to weathering/yellowing processes. Particles with black and grey hues covered percentages varying from ~8 to 12%, while all other colours totally contributed to 9–11%. In general, opaque items dominated (41–57%), while transparent debris represented ~7 to 13%. Intermediate optical properties, such as the translucent and semi-translucent ones, amounted to ~ 36–45%.

All these characteristics were used to generate specific groups (sg_is) to cross-link information for comparing the large set of data acquired in the two monitoring campaigns. It was found that collected particles were distributed in many sg_is, characterized in most of the cases by few typical frequencies. In particular, for M1 the 68% of microplastics resulted to belong to 45 sg_is whose frequency varies between 1 and 4%; for M2 the same numerosity frequencies include 88 sg_is representing the 52% of particles. For both campaigns, only one sg_i has been individuated with a frequency higher than 10% and containing 11–13% of particles.

The analysis through two diversity indexes (Shannon, *H'* and Simpson, D_s) confirmed that floating plastic debris resulted well diversified in terms of sg_is presence and that particles distribute uniformly within them. This was probably the result of different origin sources and generation processes. Additionally, a comparison between the two indexes pointed out that the structure of micro- and mesoplastic sets showed the same diversity level in both campaigns.

The proposed approach based on the typization of microplastic particles and the use of diversity indexes resulted particularly useful for the management of huge amounts of different data obtained from the characterization of microplastics collected from environmental sampling session and allowed estimating differences existing among data obtained from various sampling campaigns.

Supplementary Information The online version contains supplementary material available at https://doi.org/10.1007/s11356-021-17874-9.

Acknowledgements The authors are grateful to Madatec srl (Pessano con Bornago, Italy) for its technical support.

Author contribution D. Marchetto: conceptualization, data acquisition, data elaboration, writing and generation of figures and tables.

L. de Ferri: writing, text revision and generation of figures and tables.

A. Latella: Data acquisition.

G. Pojana: acquisition of funding, conceptualization and text revision.

Funding This study was funded by the "IPA ADRIATIC CBC PROGRAMME 2007–2013 Derelict Fishing Gear Management System in the Adriatic Region" Project Code STR/00010.

Data availability All data generated or analysed during this study are included in this article and its supplementary information files.

Declarations

Ethics approval and consent to participate Not applicable.

Consent for publication All authors agree on the presented version of the paper for publication.

Competing interests The authors declare no competing interests.

References

Abayomi OA, Range P, Al-Ghouti MA et al (2017) Microplastics in coastal environments of the Arabian Gulf. Mar Pollut Bull 124:181–188. https://doi.org/10.1016/j.marpolbul.2017.07.011

Andrady AL (2011) Microplastics in the marine environment. Mar Pollut Bull 62:1596–1605. https://doi.org/10.1016/j.marpolbul.2011.05.030

Andrady AL (2017) The plastic in microplastics: a review. Mar Pollut Bull 119:12–22. https://doi.org/10.1016/j.marpolbul.2017.01.082

Andrady AL (2015) Persistence of plastic litter in the oceans. In: Bergmann M, Gutow L, Klages M (eds) Marine Anthropogenic Litter. Springer International Publishing, Cham, pp 57–72

Andrady AL, Neal MA (2009) Applications and societal benefits of plastics. Philos Trans R Soc Lond B Biol Sci 364:1977–1984. https://doi.org/10.1098/rstb.2008.0304

Artegiani A, Paschini E, Russo A et al (1997) The Adriatic Sea general circulation. Part II: Baroclinic Circulation Structure. J Phys Oceanogr 27:1515–1532. https://doi.org/10.1175/1520-0485(1997)027%3c1515:TASGCP%3e2.0.CO;2

Arthur C, Baker H, Bamford H, et al (2008) Proceedings of the International Research Workshop on the Occurrence, Effects, and Fate of Microplastic Marine Debris, September 9–11, 2008, University of Washington Tacoma, Tacoma, WA, USA. Arthur, C., J. Baker and H. Bamford

Avio CG, Gorbi S, Regoli F (2015) Experimental development of a new protocol for extraction and characterization of microplastics in fish tissues: first observations in commercial species from Adriatic Sea. Mar Environ Res 111:18–26. https://doi.org/10.1016/j.marenvres.2015.06.014

Aytan U, Valente A, Senturk Y et al (2016) First evaluation of neustonic microplastics in Black Sea waters. Mar Environ Res 119:22–30. https://doi.org/10.1016/j.marenvres.2016.05.009

Azzarello MY, Van Vleet ES (1987) Marine birds and plastic pollution. Mar Ecol Prog Ser 37:295–303

Bakir A, Rowland SJ, Thompson RC (2014) Enhanced desorption of persistent organic pollutants from microplastics under simulated physiological conditions. Environ Pollut 185:16–23. https://doi.org/10.1016/j.envpol.2013.10.007

Barnes DKA, Galgani F, Thompson RC, Barlaz M (2009) Accumulation and fragmentation of plastic debris in global environments. Philos Trans R Soc Lond B Biol Sci 364:1985–1998. https://doi.org/10.1098/rstb.2008.0205

Beer S, Garm A, Huwer B et al (2018) No increase in marine microplastic concentration over the last three decades – a case study from the Baltic Sea. Sci Total Environ 621:1272–1279. https://doi.org/10.1016/j.scitotenv.2017.10.101

Bellafiore D, Umgiesser G, Cucco A (2008) Modeling the water exchanges between the Venice Lagoon and the Adriatic Sea. Ocean Dyn 58:397–413. https://doi.org/10.1007/s10236-008-0152-7

Bergamasco A, Gačić M (1996) Baroclinic response of the Adriatic Sea to an episode of bora wind. J Phys Oceanogr 26:1354–1369. https://doi.org/10.1175/1520-0485(1996)026%3c1354:BROTAS%3e2.0.CO;2

Blanco M, Villarroya I (2002) NIR spectroscopy: a rapid-response analytical tool. TrAC Trends Anal Chem 21:240–250. https://doi.org/10.1016/S0165-9936(02)00404-1

Botterell ZLR, Beaumont N, Dorrington T et al (2019) Bioavailability and effects of microplastics on marine zooplankton: a review. Environ Pollut 245:98–110. https://doi.org/10.1016/j.envpol.2018.10.065

Brandon J, Goldstein M, Ohman MD (2016) Long-term aging and degradation of microplastic particles: comparing in situ oceanic and experimental weathering patterns. Mar Pollut Bull 110:299–308. https://doi.org/10.1016/j.marpolbul.2016.06.048

Brower JE, Jerrold H, von Ende CN (1998) Field and laboratory methods for general ecology. Mc Graw-Hill, Boston

Brown DM, Cheng L (1981) New net for sampling the ocean surface. Mar Ecol Prog Ser 5:225–227

Browne MA, Dissanayake A, Galloway TS et al (2008) Ingested microscopic plastic translocates to the circulatory system of the mussel, Mytilus edulis (L.). Environ Sci Technol 42:5026–5031. https://doi.org/10.1021/es800249a

Browne MA, Underwood AJ, Chapman MG et al (2015) Linking effects of anthropogenic debris to ecological impacts. Proc R Soc B 282:20142929. https://doi.org/10.1098/rspb.2014.2929

Buljan M, Zore-Armanda M (1976) Oceanographic properties of the Adriatic Sea. Ocean Mar Biol Ann 14:11–98

Castillo AB, Al-Maslamani I, Obbard JP (2016) Prevalence of microplastics in the marine waters of Qatar. Mar Pollut Bull 111:260–267. https://doi.org/10.1016/j.marpolbul.2016.06.108

Cavaleri L, Bertotti L, Tescaro N (1997) The modelled wind climatology of the Adriatic Sea. Theor Appl Climatol 56:231–254. https://doi.org/10.1007/BF00866430

Chae Y, An Y-J (2017) Effects of micro- and nanoplastics on aquatic ecosystems: current research trends and perspectives. Mar Pollut Bull 124:624–632. https://doi.org/10.1016/j.marpolbul.2017.01.070

Cincinelli A, Martellini T, Guerranti C et al (2019) A potpourri of microplastics in the sea surface and water column of the Mediterranean Sea. TrAC Trends Anal Chem 110:321–326. https://doi.org/10.1016/j.trac.2018.10.026

Collignon A, Hecq J-H, Galgani F et al (2014) Annual variation in neustonic micro- and meso-plastic particles and zooplankton in the Bay of Calvi (Mediterranean–Corsica). Mar Pollut Bull 79:293–298. https://doi.org/10.1016/j.marpolbul.2013.11.023

Collignon A, Hecq J-H, Glagani F et al (2012) Neustonic microplastic and zooplankton in the North Western Mediterranean Sea. Mar Pollut Bull 64:861–864. https://doi.org/10.1016/j.marpolbul.2012.01.011

Constant M, Kerherve P, Sola J, et al (2018) Floating microplastics in the Northwestern Mediterranean Sea: temporal and spatial heterogeneities. In: Cocca M, Di Pace E, Errico ME, et al. (eds) Proceedings of the International Conference on Microplastic Pollution in the Mediterranean Sea. Springer International Publishing, Cham, pp 9–15

Cooper DA, Corcoran PL (2010) Effects of mechanical and chemical processes on the degradation of plastic beach debris on the island of Kauai. Hawaii Mar Pollut Bull 60:650–654. https://doi.org/10.1016/j.marpolbul.2009.12.026

Cózar A, Echevarría F, González-Gordillo JI et al (2014) Plastic debris in the open ocean. Proc Natl Acad Sci 111:10239–10244. https://doi.org/10.1073/pnas.1314705111

Cózar A, Sanz-Martín M, Martí E et al (2015) Plastic accumulation in the Mediterranean Sea. PLoS ONE 10:e0121762. https://doi.org/10.1371/journal.pone.0121762

Dai Z, Zhang H, Zhou Q et al (2018) Occurrence of microplastics in the water column and sediment in an inland sea affected by intensive anthropogenic activities. Environ Pollut 242:1557–1565. https://doi.org/10.1016/j.envpol.2018.07.131

de Lucia GA, Caliani I, Marra S et al (2014) Amount and distribution of neustonic micro-plastic off the western Sardinian coast (Central-Western Mediterranean Sea). Mar Environ Res 100:10–16. https://doi.org/10.1016/j.marenvres.2014.03.017

Derraik JGB (2002) The pollution of the marine environment by plastic debris: a review. Mar Pollut Bull 44:842–852. https://doi.org/10.1016/S0025-326X(02)00220-5

Di Mauro R, Kupchik MJ, Benfield MC (2017) Abundant plankton-sized microplastic particles in shelf waters of the northern Gulf of Mexico. Environ Pollut 230:798–809. https://doi.org/10.1016/j.envpol.2017.07.030

Dubaish F, Liebezeit G (2013) Suspended microplastics and black carbon particles in the Jade System, Southern North Sea. Water Air Soil Pollut 224:1352. https://doi.org/10.1007/s11270-012-1352-9

Engler RE (2012) The complex interaction between marine debris and toxic chemicals in the ocean. Environ Sci Technol 46:12302–12315. https://doi.org/10.1021/es3027105

Espinosa C, Cuesta A, Esteban MÁ (2017) Effects of dietary polyvinylchloride microparticles on general health, immune status and expression of several genes related to stress in gilthead seabream (Sparus aurata L.). Fish Shellfish Immunol 68:251–259. https://doi.org/10.1016/j.fsi.2017.07.006

European Commission. Joint Research Centre. Institute for Environment and Sustainability (2011) Marine litter : technical recommendations for the implementation of MSFD requirements. Publications Office, LU

Fahrenfeld NL, Arbuckle-Keil G, Naderi Beni N, Bartelt-Hunt SL (2019) Source tracking microplastics in the freshwater environment. TrAC Trends Anal Chem 112:248–254. https://doi.org/10.1016/j.trac.2018.11.030

Farrell P, Nelson K (2013) Trophic level transfer of microplastic: Mytilus edulis (L.) to Carcinus maenas (L.). Environ Pollut 177:1–3. https://doi.org/10.1016/j.envpol.2013.01.046

Faure F, Saini C, Potter G et al (2015) An evaluation of surface micro- and mesoplastic pollution in pelagic ecosystems of the Western Mediterranean Sea. Environ Sci Pollut Res 22:12190–12197. https://doi.org/10.1007/s11356-015-4453-3

Ferreira T, Rasband WS (2012) ImageJ User Guide - IJ 1.46

Fofonoff NP, Millard RC (1983) UNESCO Technical Papers IN Marine Science 44 - algorithms for computation of fundamental properties of seawater

Fossi MC, Marsili L, Baini M et al (2016) Fin whales and microplastics: the Mediterranean Sea and the Sea of Cortez scenarios. Environ Pollut 209:68–78. https://doi.org/10.1016/j.envpol.2015.11.022

Fossi MC, Panti C, Guerranti C et al (2012) Are baleen whales exposed to the threat of microplastics? A case study of the Mediterranean fin whale (Balaenoptera physalus). Mar Pollut Bull 64:2374–2379. https://doi.org/10.1016/j.marpolbul.2012.08.013

MC Fossi T Romeo M Baini et al 2017 Plastic debris occurrence, convergence areas and fin whales feeding ground in the Mediterranean marine protected area Pelagos sanctuary: a modeling approach Front Mar Sci 4 https://doi.org/10.3389/fmars.2017.00167

Gačić M, Kovačević V, Cosoli S et al (2009) Surface current patterns in front of the Venice Lagoon. Estuar Coast Shelf Sci 82:485–494. https://doi.org/10.1016/j.ecss.2009.02.012

Gajšt T, Bizjak T, Palatinus A et al (2016) Sea surface microplastics in Slovenian part of the Northern Adriatic. Mar Pollut Bull 113:392–399. https://doi.org/10.1016/j.marpolbul.2016.10.031

Galgani F, Hanke G, Werner S, De Vrees L (2013) Marine litter within the European Marine Strategy Framework Directive. ICES J Mar Sci 70:1055–1064. https://doi.org/10.1093/icesjms/fst122

Gambardella C, Morgana S, Ferrando S et al (2017) Effects of polystyrene microbeads in marine planktonic crustaceans. Ecotoxicol Environ Saf 145:250–257. https://doi.org/10.1016/j.ecoenv.2017.07.036

Gauci A, Deidun A, Montebello J et al (2019) Automating the characterisation of beach microplastics through the application of image analyses. Ocean Coast Manag 182:104950. https://doi.org/10.1016/j.ocecoaman.2019.104950

Geller Y (2007) Using MEMS technology for cost effective recycling of plastics. In: Dickensheets DL, Gogoi BP, Schenk H (eds) SPIE Proceedings. p 646604

GESAMP (2019) Guidelines or the monitoring and assessment of plastic litter and microplastics in the ocean. Rep Stud. No. 99. (Kershaw P.J., TurraA. and Galgani F.), (IMO/FAO/UNESCO-IOC/UNIDO/WMO/IAEA/UN/UNEP/UNDP/ISA Joint Group of Experts on the Scientific Aspects of Marine Environmental Protection)

Gewert B, Ogonowski M, Barth A, MacLeod M (2017) Abundance and composition of near surface microplastics and plastic debris in the Stockholm Archipelago, Baltic Sea. Mar Pollut Bull 120:292–302. https://doi.org/10.1016/j.marpolbul.2017.04.062

Gewert B, Plassmann MM, MacLeod M (2015) Pathways for degradation of plastic polymers floating in the marine environment. Environ Sci Process Impacts 17:1513–1521. https://doi.org/10.1039/C5EM00207A

Goldberg ED (1995) Emerging problems in the coastal zone for the twenty-first century. Mar Pollut Bull 31:152–158. https://doi.org/10.1016/0025-326X(95)00102-S

Goldberg ED (1994) Diamonds and plastics are forever? Mar Pollut Bull 28:466. https://doi.org/10.1016/0025-326X(94)90511-8

Gorokhova E (2015) Screening for microplastic particles in plankton samples: how to integrate marine litter assessment into existing monitoring programs? Mar Pollut Bull 99:271–275. https://doi.org/10.1016/j.marpolbul.2015.07.056

Green DS, Boots B, O'Connor NE, Thompson R (2017) Microplastics affect the ecological functioning of an important biogenic habitat. Environ Sci Technol 51:68–77. https://doi.org/10.1021/acs.est.6b04496

Green DS, Boots B, Sigwart J et al (2016) Effects of conventional and biodegradable microplastics on a marine ecosystem engineer (Arenicola marina) and sediment nutrient cycling. Environ Pollut 208:426–434. https://doi.org/10.1016/j.envpol.2015.10.010

Gregory MR (2009) Environmental implications of plastic debris in marine settings—entanglement, ingestion, smothering, hangers-on, hitch-hiking and alien invasions. Philos Trans R Soc Lond B Biol Sci 364:2013–2025. https://doi.org/10.1098/rstb.2008.0265

Gündoğdu S, Çevik C (2017) Micro- and mesoplastics in Northeast Levantine coast of Turkey: the preliminary results from surface samples. Mar Pollut Bull 118:341–347. https://doi.org/10.1016/j.marpolbul.2017.03.002

Guzzetti E, Sureda A, Tejada S, Faggio C (2018) Microplastic in marine organism: environmental and toxicological effects. Environ Toxicol Pharmacol 64:164–171. https://doi.org/10.1016/j.etap.2018.10.009

Hanke G, Galgani F, Werner S, et al (2013) Guidance on monitoring of marine litter in European seas. Publications Office of the European Union

Healy T, Harada K (1991) Definition and physical characteristics of the world's enclosed coastal seas. Mar Pollut Bull 23:639–644. https://doi.org/10.1016/0025-326X(91)90749-I

Helm PA (2017) Improving microplastics source apportionment: a role for microplastic morphology and taxonomy? Anal Methods 9:1328–1331. https://doi.org/10.1039/C7AY90016C

Hidalgo-Ruz V, Gutow L, Thompson RC, Thiel M (2012) Microplastics in the marine environment: a review of the methods used for identification and quantification. Environ Sci Technol 46:3060–3075. https://doi.org/10.1021/es2031505

Hirt N, Body-Malapel M (2020) Immunotoxicity and intestinal effects of nano- and microplastics: a review of the literature. Part Fibre Toxicol 17:57. https://doi.org/10.1186/s12989-020-00387-7

https://www.mareografico RETE MAREOGRAFICA NAZIONALE - HOMEPAGE. In: RETE MAREOGRAFICA Naz. - HOMEPAGE. https://www.mareografico.it/. Accessed 29 Jul 2021

https://www.venezia.isprambiente.it/rete-meteo-mareografica ISPRA Servizio Laguna di Venezia - Rete meteo-mareografica. In: ISPRA Serv. Laguna Venezia - Rete Meteo-Mareografica. https://www.venezia.isprambiente.it/rete-meteo-mareografica. Accessed 29 Jul 2021

Isobe A, Kubo K, Tamura Y et al (2014) Selective transport of microplastics and mesoplastics by drifting in coastal waters. Mar Pollut Bull 89:324–330. https://doi.org/10.1016/j.marpolbul.2014.09.041

Isobe A, Uchida K, Tokai T, Iwasaki S (2015) East Asian seas: a hot spot of pelagic microplastics. Mar Pollut Bull 101:618–623. https://doi.org/10.1016/j.marpolbul.2015.10.042

Jayaraman K (1999) A statistical manual for forestry research. In: www.fao.org. http://www.fao.org/3/x6831e/x6831e14.htm. Accessed 28 Feb 2021

Jeong C-B, Won E-J, Kang H-M et al (2016) Microplastic size-dependent toxicity, oxidative stress induction, and p-JNK and p-p38 activation in the Monogonont Rotifer (Brachionus koreanus). Environ Sci Technol 50:8849–8857. https://doi.org/10.1021/acs.est.6b01441

Jin Y, Xia J, Pan Z et al (2018) Polystyrene microplastics induce microbiota dysbiosis and inflammation in the gut of adult zebrafish. Environ Pollut 235:322–329. https://doi.org/10.1016/j.envpol.2017.12.088

Kourafalou VH (2001) River plume development in semi-enclosed Mediterranean regions: North Adriatic Sea and Northwestern Aegean Sea. J Mar Syst 30:181–205. https://doi.org/10.1016/S0924-7963(01)00058-6

Krajcar V (2003) Climatology of geostrophic currents in the Northern Adriatic. Geofizika 20:105–114

Kukulka T, Proskurowski G, Morét-Ferguson S et al (2012) The effect of wind mixing on the vertical distribution of buoyant plastic debris. Geophys Res Lett 39:L07601. https://doi.org/10.1029/2012GL051116

Laist DW (1987) Overview of the biological effects of lost and discarded plastic debris in the marine environment. Mar Pollut Bull 18:319–326. https://doi.org/10.1016/S0025-326X(87)80019-X

Laist DW (1997) Impact of marine debris: entanglement of marine life in marine debris including a comprehensive list of species with entanglement and ingestion records. In: Coe JM, Rogers D (eds) Marine Debris. Sources, Impacts and Solution. Springer-Verlag, New York, NY

Lambert S, Wagner M (2016) Formation of microscopic particles during the degradation of different polymers. Chemosphere 161:510–517. https://doi.org/10.1016/j.chemosphere.2016.07.042

Large WG, Pond S (1981) Open ocean momentum flux measurements in moderate to strong winds. J Phys Oceanogr 11:324–336. https://doi.org/10.1175/1520-0485(1981)011%3c0324:OOMFMI%3e2.0.CO;2

Lattin GL, Moore CJ, Zellers AF et al (2004) A comparison of neustonic plastic and zooplankton at different depths near the southern California shore. Mar Pollut Bull 49:291–294. https://doi.org/10.1016/j.marpolbul.2004.01.020

Lei L, Wu S, Lu S et al (2018) Microplastic particles cause intestinal damage and other adverse effects in zebrafish Danio rerio and nematode Caenorhabditis elegans. Sci Total Environ 619–620:1–8. https://doi.org/10.1016/j.scitotenv.2017.11.103

LeMoine CMR, Kelleher BM, Lagarde R et al (2018) Transcriptional effects of polyethylene microplastics ingestion in developing zebrafish (Danio rerio). Environ Pollut 243:591–600. https://doi.org/10.1016/j.envpol.2018.08.084

Limonta G, Mancia A, Benkhalqui A et al (2019) Microplastics induce transcriptional changes, immune response and behavioral alterations in adult zebrafish. Sci Rep 9:15775. https://doi.org/10.1038/s41598-019-52292-5

Lithner D, Larsson Å, Dave G (2011) Environmental and health hazard ranking and assessment of plastic polymers based on chemical composition. Sci Total Environ 409:3309–3324. https://doi.org/10.1016/j.scitotenv.2011.04.038

Lusher AL, McHugh M, Thompson RC (2013) Occurrence of microplastics in the gastrointestinal tract of pelagic and demersal fish from the English Channel. Mar Pollut Bull 67:94–99. https://doi.org/10.1016/j.marpolbul.2012.11.028

T Maes MD Meulen Van der LI Devriese et al 2017 Microplastics baseline surveys at the water surface and in sediments of the North-East Atlantic Front Mar Sci 4 https://doi.org/10.3389/fmars.2017.00135

E Martí C Martin A Cózar CM Duarte 2017 Low abundance of plastic fragments in the surface waters of the Red Sea Front Mar Sci 4 https://doi.org/10.3389/fmars.2017.00333

Martí E, Martin C, Galli M et al (2020) The colors of the ocean plastics. Environ Sci Technol 54:6594–6601. https://doi.org/10.1021/acs.est.9b06400

Mauri E, Poulain P-M (2001) Northern Adriatic Sea surface circulation and temperature/pigment fields in September and October 1997. J Mar Syst 29:51–67. https://doi.org/10.1016/S0924-7963(01)00009-4

McCamy CS, Marcus H, Davidson JG (1976) A color-rendition chart. J Appl Photogr Eng 2:95–99

McKinney FK (2007a) Geography of the Northern Adriatic Sea. The Northern Adriatic Ecosystem: Deep Time in a Shallow Sea. Columbia University Press, New York, NY, pp 29–43

McKinney FK (2007b) Physical oceanography. The Northern Adriatic Ecosystem: Deep Time in a Shallow Sea. Columbia University Press, New York, NY, pp 61–85

McKinney FK (2007c) Nutrients and pelagic biology. The Northern Adriatic Ecosystem: Deep Time in a Shallow Sea. Columbia University Press, New York, NY, pp 86–121

Michida Y, Chavanich S, Chiba S, et al (2019) Guidelines for harmonizing ocean surface microplastic monitoring methods. Version 1.1. Ministry of the Environment, Japan

Millero FJ, Poisson A (1981) International one-atmosphere equation of state of seawater. Deep Sea Res Part Oceanogr Res Pap 28:625–629. https://doi.org/10.1016/0198-0149(81)90122-9

Moore CJ (2008) Synthetic polymers in the marine environment: a rapidly increasing, long-term threat. Environ Res 108:131–139. https://doi.org/10.1016/j.envres.2008.07.025

Moore CJ, Moore SL, Leecaster MK, Weisberg SB (2001) A comparison of plastic and plankton in the North Pacific Central Gyre. Mar Pollut Bull 42:1297–1300. https://doi.org/10.1016/S0025-326X(01)00114-X

Mosetti F, Lavenia A (1969) Ricerche oceanografiche in Adriatico. Boll Geofis Teor Ed Appl 11:191–218

Mueller R-J (2006) Biological degradation of synthetic polyesters—enzymes as potential catalysts for polyester recycling. Process Biochem 41:2124–2128. https://doi.org/10.1016/j.procbio.2006.05.018

Ogata Y, Takada H, Mizukawa K et al (2009) International pellet watch: global monitoring of persistent organic pollutants (POPs) in coastal waters. 1. Initial phase data on PCBs, DDTs, and HCHs. Mar Pollut Bull 58:1437–1446. https://doi.org/10.1016/j.marpolbul.2009.06.014

Ohtake Y, Kobayashi T, Asabe H et al (1998a) Oxidative degradation and molecular weight change of LDPE buried under bioactive soil for 32–37 years. J Appl Polym Sci 70:1643–1648. https://doi.org/10.1002/(SICI)1097-4628(19981128)70:9%3c1643::AID-APP1%3e3.0.CO;2-V

Ohtake Y, Kobayashi T, Asabe H, Murakami N (1998b) Studies on biodegradation of LDPE — observation of LDPE films scattered in agricultural fields or in garden soil. Polym Degrad Stab 60:79–84. https://doi.org/10.1016/S0141-3910(97)00032-3

Orlić M (1989) Salinity of the North Adriatic: a fresh look at some old data. Boll Oceanol Teor E Appl 7:219–228

Orlić M, Kuzmić M, Pasarić Z (1994) Response of the Adriatic Sea to the bora and sirocco forcing. Cont Shelf Res 14:91–116. https://doi.org/10.1016/0278-4343(94)90007-8

Pedrotti ML, Petit S, Elineau A et al (2016) Changes in the floating plastic pollution of the Mediterranean Sea in relation to the distance to land. PLoS ONE 11:e0161581. https://doi.org/10.1371/journal.pone.0161581

Pegram JE, Andrady AL (1989) Outdoor weathering of selected polymeric materials under marine exposure conditions. Polym Degrad Stab 26:333–345. https://doi.org/10.1016/0141-3910(89)90112-2

Pitt JA, Kozal JS, Jayasundara N et al (2018) Uptake, tissue distribution, and toxicity of polystyrene nanoparticles in developing zebrafish (Danio rerio). Aquat Toxicol 194:185–194. https://doi.org/10.1016/j.aquatox.2017.11.017

Poulain P-M (2001) Adriatic Sea surface circulation as derived from drifter data between 1990 and 1999. J Mar Syst 29:3–32. https://doi.org/10.1016/S0924-7963(01)00007-0

Poulain P-M (1999) Drifter observations of surface circulation in the Adriatic Sea between December 1994 and March 1996. J Mar Syst 20:231–253. https://doi.org/10.1016/S0924-7963(98)00084-0

Prokić MD, Radovanović TB, Gavrić JP, Faggio C (2019) Ecotoxicological effects of microplastics: examination of biomarkers, current state and future perspectives. TrAC Trends Anal Chem 111:37–46. https://doi.org/10.1016/j.trac.2018.12.001

Pruter AT (1987) Sources, quantities and distribution of persistent plastics in the marine environment. Mar Pollut Bull 18:305–310. https://doi.org/10.1016/S0025-326X(87)80016-4

Qu X, Su L, Li H et al (2018) Assessing the relationship between the abundance and properties of microplastics in water and in mussels. Sci Total Environ 621:679–686. https://doi.org/10.1016/j.scitotenv.2017.11.284

Raicich F (1994) Note on the flow rates of the Adriatic Rivers. Consiglio Nazionale delle Ricerche - Istituto Sperimentale Talassografico

Reisser J, Shaw J, Wilcox C et al (2013) Marine plastic pollution in waters around Australia: characteristics, concentrations, and pathways. PLoS ONE 8:e80466. https://doi.org/10.1371/journal.pone.0080466

Ribeiro F, Garcia AR, Pereira BP et al (2017) Microplastics effects in Scrobicularia plana. Mar Pollut Bull 122:379–391. https://doi.org/10.1016/j.marpolbul.2017.06.078

Rizzoli PM, Bergamasco A (1983) The dynamics of the coastal region of the Northern Adriatic Sea. J Phys Oceanogr 13:1105–1130. https://doi.org/10.1175/1520-0485(1983)013%3c1105:TDOTCR%3e2.0.CO;2

Rochman CM, Hoh E, Hentschel BT, Kaye S (2013) Long-term field measurement of sorption of organic contaminants to five types of plastic pellets: implications for plastic marine debris. Environ Sci Technol 47:1646–1654. https://doi.org/10.1021/es303700s

Ruiz-Orejón LF, Sardá R, Ramis-Pujol J (2016) Floating plastic debris in the Central and Western Mediterranean Sea. Mar Environ Res 120:136–144. https://doi.org/10.1016/j.marenvres.2016.08.001

Sadri SS, Thompson RC (2014) On the quantity and composition of floating plastic debris entering and leaving the Tamar Estuary, Southwest England. Mar Pollut Bull 81:55–60. https://doi.org/10.1016/j.marpolbul.2014.02.020

Setälä O, Fleming-Lehtinen V, Lehtiniemi M (2014) Ingestion and transfer of microplastics in the planktonic food web. Environ Pollut 185:77–83. https://doi.org/10.1016/j.envpol.2013.10.013

Setälä O, Magnusson K, Lehtiniemi M, Norén F (2016a) Distribution and abundance of surface water microlitter in the Baltic Sea: a comparison of two sampling methods. Mar Pollut Bull 110:177–183. https://doi.org/10.1016/j.marpolbul.2016.06.065

Setälä O, Norkko J, Lehtiniemi M (2016b) Feeding type affects microplastic ingestion in a coastal invertebrate community. Mar Pollut Bull 102:95–101. https://doi.org/10.1016/j.marpolbul.2015.11.053

Shannon CE (1948) A mathematical theory of communication. Bell Syst Tech J 27:379–423. https://doi.org/10.1002/j.1538-7305.1948.tb01338.x

Shaw DG, Day RH (1994) Colour- and form-dependent loss of plastic micro-debris from the North Pacific Ocean. Mar Pollut Bull 28:39–43. https://doi.org/10.1016/0025-326X(94)90184-8

Simpson EH (1949) Measurement of diversity. Nature 163:688–688. https://doi.org/10.1038/163688a0

Singh B, Sharma N (2008) Mechanistic implications of plastic degradation. Polym Degrad Stab 93:561–584. https://doi.org/10.1016/j.polymdegradstab.2007.11.008

Song YK, Hong SH, Jang M et al (2014) Large accumulation of micro-sized synthetic polymer particles in the sea surface microlayer. Environ Sci Technol 48:9014–9021. https://doi.org/10.1021/es501757s

Soper D (2018) Free Statistics Calculators - Home. In: www.danielsoper. https://www.danielsoper.com/statcalc/. Accessed 28 Feb 2021

Sorak D, Herberholz L, Iwascek S et al (2012) New developments and applications of handheld Raman, mid-infrared, and near-infrared spectrometers. Appl Spectrosc Rev 47:83–115. https://doi.org/10.1080/05704928.2011.625748

Suaria G, Avio CG, Mineo A et al (2016) The Mediterranean Plastic Soup: synthetic polymers in Mediterranean surface waters. Sci Rep 6:37551. https://doi.org/10.1038/srep37551

Tamminga M, Hengstmann E, Fischer EK (2018) Microplastic analysis in the South Funen Archipelago, Baltic Sea, implementing manta trawling and bulk sampling. Mar Pollut Bull 128:601–608. https://doi.org/10.1016/j.marpolbul.2018.01.066

ter Halle A, Ladirat L, Gendre X et al (2016) Understanding the fragmentation pattern of marine plastic debris. Environ Sci Technol 50:5668–5675. https://doi.org/10.1021/acs.est.6b00594

ter Halle A, Ladirat L, Martignac M et al (2017) To what extent are microplastics from the open ocean weathered? Environ Pollut 227:167–174. https://doi.org/10.1016/j.envpol.2017.04.051

Teuten EL, Rowland SJ, Galloway TS, Thompson RC (2007) Potential for plastics to transport hydrophobic contaminants. Environ Sci Technol 41:7759–7764. https://doi.org/10.1021/es071737s

Thompson RC, Swan SH, Moore CJ, vom Saal FS (2009) Our plastic age. Philos Trans R Soc Lond B Biol Sci 364:1973–1976. https://doi.org/10.1098/rstb.2009.0054

Tokai T, Uchida K, Kuroda M, Isobe A (2021) Mesh selectivity of neuston nets for microplastics. Mar Pollut Bull 165:112111. https://doi.org/10.1016/j.marpolbul.2021.112111

Trenberth KE, Large WG, Olson JG (1990) The mean annual cycle in global ocean wind stress. J Phys Oceanogr 20:1742–1760. https://doi.org/10.1175/1520-0485(1990)020%3c1742:TMACIG%3e2.0.CO;2

Tunçer S, Artüz OB, Demirkol M, Artüz ML (2018) First report of occurrence, distribution, and composition of microplastics in surface waters of the Sea of Marmara, Turkey. Mar Pollut Bull 135:283–289. https://doi.org/10.1016/j.marpolbul.2018.06.054

United States. Army. Corps of Engineers, Coastal Engineering Research Center (U.S.) (1984) Shore protection manual. Vicksburg, Miss. : Dept. of the Army, Waterways Experiment Station, Corps of Engineers, Coastal Engineering Research Center ; Washington, DC : For sale by the Supt. of Docs., U.S. G.P.O.

Van Cauwenberghe L, Janssen CR (2014) Microplastics in bivalves cultured for human consumption. Environ Pollut 193:65–70. https://doi.org/10.1016/j.envpol.2014.06.010

van der Hal N, Ariel A, Angel DL (2017) Exceptionally high abundances of microplastics in the oligotrophic Israeli Mediterranean coastal waters. Mar Pollut Bull 116:151–155. https://doi.org/10.1016/j.marpolbul.2016.12.052

Veneman WJ, Spaink HP, Brun NR et al (2017) Pathway analysis of systemic transcriptome responses to injected polystyrene particles in zebrafish larvae. Aquat Toxicol 190:112–120. https://doi.org/10.1016/j.aquatox.2017.06.014

Vianello A, Da Ros L, Boldrin A et al (2018) First evaluation of floating microplastics in the Northwestern Adriatic Sea. Environ Sci Pollut Res 25:28546–28561. https://doi.org/10.1007/s11356-018-2812-6

Wang T, Zou X, Li B et al (2018) Microplastics in a wind farm area: a case study at the Rudong Offshore Wind Farm, Yellow Sea, China. Mar Pollut Bull 128:466–474. https://doi.org/10.1016/j.marpolbul.2018.01.050

Wright SL, Kelly FJ (2017) Plastic and human health: a micro issue? Environ Sci Technol 51:6634–6647. https://doi.org/10.1021/acs.est.7b00423

Wright SL, Thompson RC, Galloway TS (2013) The physical impacts of microplastics on marine organisms: a review. Environ Pollut 178:483–492. https://doi.org/10.1016/j.envpol.2013.02.031

Yonkos LT, Friedel EA, Perez-Reyes AC et al (2014) Microplastics in four estuarine rivers in the Chesapeake Bay, U.S.A. Environ Sci Technol 48:14195–14202. https://doi.org/10.1021/es5036317

Yu P, Liu Z, Wu D et al (2018) Accumulation of polystyrene microplastics in juvenile Eriocheir sinensis and oxidative stress effects in the liver. Aquat Toxicol 200:28–36. https://doi.org/10.1016/j.aquatox.2018.04.015

Zavatarelli M, Baretta JW, Baretta-Bekker JG, Pinardi N (2000) The dynamics of the Adriatic Sea ecosystem: an idealized model study. Deep Sea Res Part Oceanogr Res Pap 47:937–970. https://doi.org/10.1016/S0967-0637(99)00086-2

Zeri C, Adamopoulou A, Bojanić Varezić D et al (2018) Floating plastics in Adriatic waters (Mediterranean Sea): from the macro- to the micro-scale. Mar Pollut Bull 136:341–350. https://doi.org/10.1016/j.marpolbul.2018.09.016

Zhang H (2017) Transport of microplastics in coastal seas. Estuar Coast Shelf Sci 199:74–86. https://doi.org/10.1016/j.ecss.2017.09.032

Zhang W, Zhang S, Wang J et al (2017) Microplastic pollution in the surface waters of the Bohai Sea, China. Environ Pollut 231:541–548. https://doi.org/10.1016/j.envpol.2017.08.058

Zhao S, Zhu L, Wang T, Li D (2014) Suspended microplastics in the surface water of the Yangtze Estuary System, China: first observations on occurrence, distribution. Mar Pollut Bull 86:562–568. https://doi.org/10.1016/j.marpolbul.2014.06.032

Zhu L, Bai H, Chen B et al (2018) Microplastic pollution in North Yellow Sea, China: observations on occurrence, distribution and identification. Sci Total Environ 636:20–29. https://doi.org/10.1016/j.scitotenv.2018.04.182

Zirino A, Elwany H, Neira C et al (2014) Salinity and its variability in the Lagoon of Venice, 2000–2009. Adv Oceanogr Limnol 5:41–59. https://doi.org/10.1080/19475721.2014.900113

Zorè M (1956) On gradient currents in the Adriatic Sea. Acta Adriat 8:1–38

Zore-Armanda M, Gačić M (1987) Effects of bura on the circulation in the North Adriatic. Ann Geophys 5:93–102

(2015) Fetch and depth limited waves, USGS.html. In: GitHub. https://github.com/csherwood-usgs/jsed. Accessed 28 Feb 2021

(IJ 1.46) ImageJ. https://imagej.nih.gov/ij/. Accessed 28 Feb 2021